Diplomarbeit

EFFECTS OF BEDREST IMMOBILIZATION ON VASCULAR FUNCTION

eingereicht von

Robin Hasso

zur Erlangung des akademischen Grades

Doktor der gesamten Heilkunde

(Dr. med. univ.)

an der

Medizinischen Universität Graz

ausgeführt am

Institut für Physiologie

unter der Anleitung von

Assoz.-Prof. Priv.-Doz. Dr.med. Nandu Goswami, PhD.

Graz, 25.4.2018

Eidesstattliche Erklärung

Ich erkläre ehrenwörtlich, dass ich die vorliegende Arbeit selbstständig und ohne fremde Hilfe verfasst habe, andere als die angegebenen Quellen nicht verwendet habe und die den benutzten Quellen wörtlich oder inhaltlich entnommenen Stellen als solche kenntlich gemacht habe.

Graz, am 25.4.2018 *Robin Hasso eh*

Acknowledgements

First and foremost I would like to thank my supervisor Dr. Nandu Goswami. Not only for presenting me with this subject and guiding me along the way, but especially for introducing me to the world of spaceflight medicine.
Many thanks also to his team at the Institut für Physiologie for their help.

I'd like to express my gratitude to the investigators at MEDES, Dr. Andrew Blaber and his team, for their help and the time in Toulouse.

Thank you Tijs for all your support and for adventurously teaching me how to use the fundus camera.

Especially big thanks to all my friends and family for keeping up with me all that time.

Abstract

Background: Cardiovascular deconditioning due to weightlessness is a major concern regarding long-term human spaceflight. Prolonged stay in a microgravity environment also causes a sometimes irreversible degradation in vision. 6° head down tilt bedrest (HDBR) has been established to simulate and study the effects of microgravity on earth.
Retinal imaging offers a non-invasive and easily reproducible in-vivo depiction of the eye's microvasculature to study changes in retinal vascular function during HDBR.
The aim of this study is to assess the changes in microvascular function during HDBR by analyzing changes in central retinal vessel diameter via fundus photography.
Methods: Data was collected during an ESA long-term bedrest campaign at MEDES space clinic in Toulouse. Retinal vascular images were obtained from ten healthy male subjects using a non-mydriatic, handheld fundus camera. Data collection took place two days prior to bedrest (BDC-2, baseline data collection) as well as on day 1, 8, 16 and 29 of HDBR (HDT01, HDT08, HDT16, HDT29, head-down tilt). Software image analysis was used to calculate central retinal arterial and venous equivalents (CRAE, CRVE) as well as arterio-venous ratio (AVR). Paired t-test was used to compare results between sampling time points. A p-value less than 0.05 was considered statistically significant.
Results: The average central retinal vessel diameters were 128.78 ± 10.65µm (CRAE) and 197.07 ±13.56µm (CRVE), respectively. On the first day of bedrest (HDT01) no significant changes took place compared to the baseline (BDC-2). In comparison to HDT01 statistically significant changes happened to CRAE on HDT08 (125.41 ± 10.90, $p = 0.007$) and on HDT29 (126.80 ± 10.05, $p = 0.011$) and to CRVE on HDT29 (191.89 ± 11.90, $p = 0.003$). AVR showed no significant changes over the course of the study, averaging at 0.65 ± 0.04.
Discussion: These results suggest that head down bedrest influences central retinal vessel diameter. Specifically, bedrest confinement leads to significant decreases in both central retinal artery and vein equivalent over the course of the study. These changes could be attributed to a myogenic response to the increased hydrostatic pressure caused by a cephalad-fluid shift induced by 6 degree head down bedrest. To my knowledge no previous study that has examined vascular changes in the retina over 60 days of bedrest immobilization.

Zusammenfassung

Hintergrund: Die Dekonditionierung des kardiovaskulären Systems ist eine der großen Hürden der bemannten Raumfahrt. Des Weiteren führen längere Aufenthalte in der Schwerelosigkeit unter Umständen zu einer irreversiblen Visusverschlechterung. Um Schwerelosigkeit zu simulieren und ihre Auswirkungen zu erforschen, wurde das Modell der Bettruhe bei 6° Kopftieflage (HDBR, head down bedrest) entwickelt.
Die Fundusfotografie bietet die Möglichkeit, die Gefäße des Augenhintergrunds nicht-invasiv und reproduzierbar in vivo darzustellen, um die Auswirkungen von HDBR auf die Gefäße der Retina zu untersuchen. Ziel dieser Arbeit ist es, Veränderungen in der Mikrozirkulation des Auges während HDBR zu erforschen. Dies geschieht durch Analyse der Vasa centrales retinae mittels Fundusfotografie.
Methoden: Die Daten wurden während einer Langzeit-HDBR-Studie der ESA an der Weltraumklinik MEDES in Toulouse erhoben. Die retinale Gefäßanalyse erfolgte mit einer nicht-mydriatischen, portablen Funduskamera an zehn gesunden, männlichen Probanden. Die Datenerhebung fand zwei Tage vor der Bettruhe, (BDC-2, baseline data collection) sowie am ersten, achten, 16. und 29. Tag der Bettruhe statt (HDT01, HDT08, HDT16, HDT29, head-down tilt). Central retinal arterial equivalent (CRAE) und central retinal venous equivalent (CRVE) sowie der ateriovenöse Quotient (AVR, arterio-venous ratio) wurden durch softwaregestützte Bildanalyse ermittelt. Die Ergebnisse der einzelnen Messungen wurden mittels abhängigem T-Test verglichen, wobei ein p-Wert kleiner 0,05 als statistisch signifikant betrachtet wurde.
Resultate: Die durchschnittlichen Gefäßdurchmesser betrugen 128,78 ± 10,65µm (CRAE) bzw. 197,07 ±13,56µm (CRVE). Verglichen mit der Baseline ergaben sich am ersten Tag der Bettruhe keine signifikanten Veränderungen. Im Vergleich mit HDT01 sank am achten Tag (HDT08) CRAE signifikant (125,41 ± 10,90, p = 0,007), am 29. Tag (HDT29) nahmen sowohl CRAE (126,80 ± 10,05, p = 0,011) als auch CRVE (191,89 ± 11,90, p = 0,003) signifikant ab. AVR zeigte im Laufe der Studie keine signifikante Veränderung, der Durchschnittwert betrug 0,65 ± 0,04.
Diskussion: Die Resultate legen einen Einfluss von head-down bedrest auf den Durchmesser der Vasa centrales retinae nahe. Bettruhe führt zu einer signifikanten Abnahme des Durchmessers sowohl der A. centralis retinae als auch der V. centralis retinae. Diese Veränderungen könnten auf eine myogene Antwort der Gefäße auf den erhöhten hydrostatischen Druck zurückgeführt werden. Dieser ergibt sich durch eine

Flüssigkeitsverschiebung in Richtung Kopf und Oberkörper aufgrund der sechs Grad Kopftieflage. Meines Wissens gibt es bislang keine Studie, die die Veränderungen der retinalen Gefäße während sechzigtägiger Bettruhe in Kopftieflage untersucht hätte.

Table of Contents

Abbreviations

ANS	Autonomic nervous system
AVR	Arterio-venous ratio
BMD	Bone Mineral Density
cAMP	Cyclic adenosine monophosphate
BMI	Body mass index
cGMP	Cyclic guanosine monophosphate
CRA	Central retinal artery
CRAE	Central retinal artery equivalent
CRV	Central retinal vein
CRVE	Central retinal vein equivalent
DLR	Deutsches Zentrum für Luft- und Raumfahrt
ECG	Electrocardiography
eNOS	Endothelial NO-synthase
ESA	European Space Agency
FMD	Flow mediated dilation
HDBR	Head down bedrest
HDT	Head down tilt
ICP	Intracranial pressure
IOP	Intraocular pressure
LTBR	Long term bedrest
MAP	Mean arterial blood pressure
MEDES	Institute for Space Medicine and Physiology
NA	Noradrenaline
NO	Nitric oxide
pCO_2	Partial pressure of carbon dioxide
pO_2	Partial pressure of oxygen
SBP	Systolic blood pressure
SD	Standard deviation
VEGF	Vascular endothelial growth factor
VIIP	Visual impairment/intracranial pressure syndrome
ZARM	Zentrum für Angewandte Raumfahrttechnologie und Mikrogravitation

List of figures

List of tables

I. INTRODUCTION

Bedrest immobilization is a major problem in today's healthcare and is responsible for both physical and physiological deconditioning. While bedrest plays an important role in recovering from illness or injury and it can indeed promote healing, being immobilized for too long poses risks and problems on its own, especially when it is time to leave the bed again. Without the constant load of one's body weight, the muscular-skeletal system will suffer from deconditioning. The bones lose their density and the muscles decrease in mass. The cardio-vascular system deconditions as well, making it hard to maintain blood pressure. Without the ability to support their body weight and to maintain proper homeostasis, patients trying to recover from extended periods of bedrest will find it difficult to do so. They will feel dizzy and insecure when standing up. This puts them at risk of falls, which will again call for bedrest to recover from said falls. People who are especially prone to this vicious cycle are the elderly. They are already at a higher risk of injuries due to falls and many of them also take medication already interfering with their blood pressure. Considering the increasing age of our society and the number of patients undergoing bedrest in our hospitals and nursing homes, a deeper understanding of the effects that long term bedrest immobilization has on the human physiology is of great importance [1, 2].

Interestingly enough, another group of people suffering from conditions very similar to that of an immobilized patient are astronauts.

I.1 Gravity and spaceflight

When returning to earth after an extended stay in space, astronauts find it difficult to stand upright, because they have problems supporting their body weight and maintaining blood pressure [3]. This is because both astronauts and immobilized patients don't have to fight gravity.

The earth's mass of about $5.97*10^{24}$ kg produces a gravitational field pulling everything within it towards earth. Mathematically, it will be drawn to earth's center of mass, i.e. earth's core, but naturally the surface of earth will stop it long before reaching the core. So effectively everything within earth's gravitational grasp will be pulled towards the ground, a direction generally referred to as 'down'. To maintain upright posture and stop a human body from being pulled to the ground, the muscles and bones have to counteract that gravitational force. They have to exert a force on the ground. (And, according to Newton's third law of motion, the ground has to exert the same but opposite force on the body.) It is

this force we perceive as weight. Weightlessness is not the absence of gravity, but rather the absence of a sensation of weight. A spacecraft orbiting the earth is still very deep within earth's gravitational field. At an altitude of 400km above sea level (the altitude of the International Space Station) earth's gravitational acceleration is still about 8.7m/s², compared to the conventional standard of 9.81m/s² on the surface of the earth [4]. It is the absence of a ground to push against, that makes the spaceship and everything in it experience weightlessness. The amount of experienced gravity (i.e. weight) is called the g-force or sometimes g-load. A force of 1g equals the weight force on earth's surface. Increasing the g-force increases an object's weight, decreasing the g-force decreases the weight up to a point of weightlessness or zero-g. Another somewhat confusing term for this state of weightlessness is microgravity.

I.1.1 Physiological deconditioning in weightlessness

A human aboard a spacecraft will suffer various physiological changes because of weightlessness. Without the need to support the body weight, the muscles lose mass and the bones decrease in density. Especially prone to this muscle deterioration are the so-called antigravity muscles, including the calf muscles, the quadriceps and the muscles of the back and neck. Without regular exercise these muscles would deteriorate and lose up to 20% of their mass within only 5-11 days in space [5–7].

Similarly, the weight supporting bones in the legs, the pelvis and the spine will suffer the most from spaceflight osteopenia, a condition comparable to osteoporosis. The rate of bone loss for elderly men and women on earth is about 1-2% of Bone Mineral Density (BMD) per year, whereas astronauts will lose an average of 1% of BMD per month [8, 9].

This loss in bone density not only increases the risk of fractures, but also raises the blood calcium levels, leading to hypercalcemia, which may result in calcification of soft tissue and kidney stone formation [9, 10].

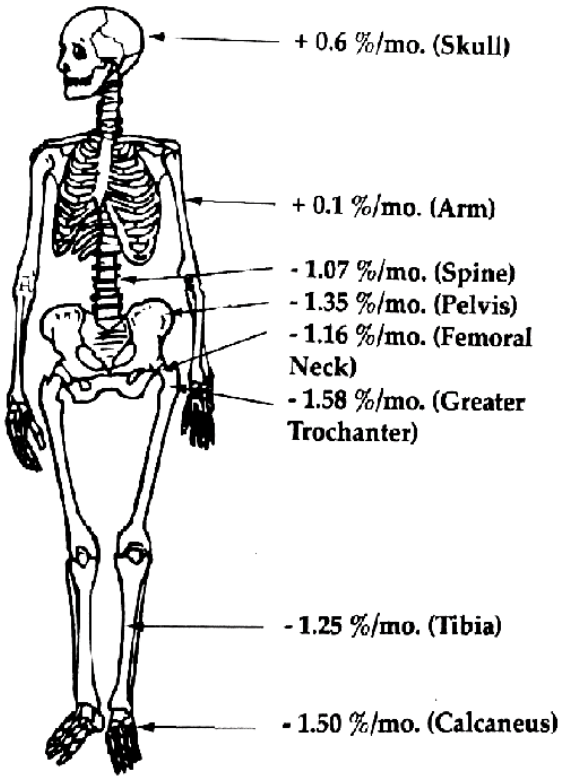

Fig. I.1: Average loss in BMD during spaceflight.
Modified from https://qph.ec.quoracdn.net/main-qimg-20319110c76b9231089532d1c24fd2c4

Another notable change can be observed in the way fluids distribute throughout the human body. On earth, blood pools in the lower extremities and the heart has to work against gravity to maintain sufficient blood pressure to perfuse the brain. Upon entering microgravity the blood distributes evenly throughout the body, leading to a cephalad fluid shift [11]. This will result in facial edema and congested sinuses frequently seen in astronauts. It also reduces the work the heart has to do to maintain cerebral blood flow. In reaction the plasma volume is decreased up to 20% and the heart atrophies. When returning to earth, the blood is pulled to the lower extremities again and the heart is too weak to maintain blood pressure. This results in orthostatic intolerance in astronauts returning from space [12].

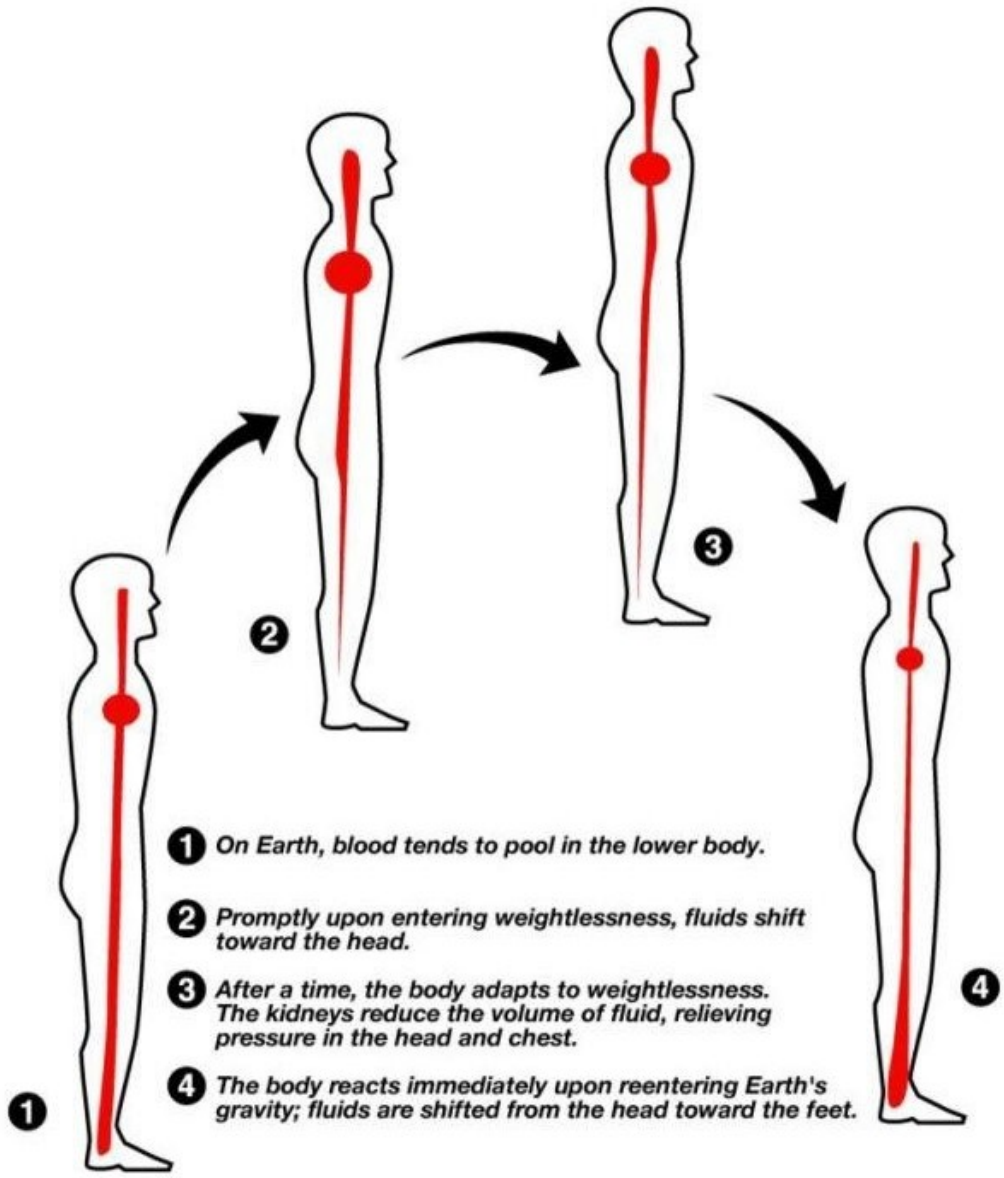

Fig. I.2: Fluid distribution and cardiac output pre-, during and post-flight.
Modified from http://img.medscape.com/article/735/035/735035-fig3.jpg

While the deconditioning of the muscular-skeletal system and orthostatic intolerance due to cardiovascular remodeling probably are the most prominent problems astronauts have to struggle with due to weightlessness, there certainly are many other difficulties to overcome. They include changes in the water and mineral balance, changes in proprioception, increased intracranial pressure and changes to the eye and vision.
To further understand the changes of microgravity on humans, more research is necessary. Although best performed aboard a spacecraft in orbit, there naturally are some restrictions to research in the environment of outer space. The costs of manned space travel and the small number of trained astronauts and manned launches make it virtually impossible to carry out all necessary research in space. There are, however, various ways to simulate microgravity on earth.

I.1.2 Simulation of microgravity

As stated above, an object is in a state of weightlessness when earth's gravitational pull is the only force acting upon it. When air resistance is not taken into account, a falling object is in such a state. An object orbiting earth is essentially in a free fall around the planet. So the easiest way to simulate microgravity is by simply dropping things. Space agencies use this mechanism in drop towers or tubes. The European Space Agency's ZARM (Zentrum für Angewandte Raumfahrttechnologie und Mikrogravitation) facility in Bremen has a drop tower of 146 meters height while the US space agency NASA uses a tube extending 155 meters underground.
The drop chamber is evacuated to eliminate the effects of air resistance. The experiments being dropped at these facilities experience microgravity for 9.3s (ESA) and 5.2s (NASA) respectively [13, 14].
The longer times at the ZARM facility are achieved by catapulting the experiment up the tower, doubling the free fall distance. Even though moving upwards, the only force acting on the experiment is gravity.

A more advanced method of studying the effects of microgravity are parabolic flights. An aircraft flying up and down following a parabolic flight path will put its passengers and cargo under different g-loads during different parts of the flight. ESA uses a specially fitted Airbus A310 for its parabolic flight experiments [15].
While on the ascending branch of the parabola everything inside the plane will experience forces up to 2g, twice earth's gravity. Once a sufficient height has been reached the pilot stops accelerating and pitching up. The plane is now essentially in free fall along the top of the parabola and everything inside will experience no gravitational pull at all. After about 20 seconds of microgravity the plane has to start pitching up again, increasing the g-load on the passengers and cargo and possibly preparing for another ascend. During one flight campaign, ESA typically performs 30 periods of weightlessness per flight with three flights conducted over the course of a week. Flight campaigns are usually performed twice a year. Slight arrangements to the flightpath also make it possible to simulate the gravity on the moon or mars [15, 16].

While these methods are used to perform short period experiments, test mission equipment or train astronauts, experiments studying mid or long term effects of microgravity are not

possible. To study these effects on human physiology, head-down bedrest (HDBR) has been established.

I.1.3 Head-down bedrest

Head-down bedrest (HDBR) is an effective way to simulate the long term effects of weightlessness on earth. The effects of immobilization are comparable to those of microgravity on the human physiology. The mechanical unloading of muscle and bone while lying in bed produces similar results to what we observe in astronauts in space [12, 17, 18]. Tilting the bed head down prevents the blood from pooling in the lower extremities and leads to a fluid shift towards the upper body, which is also observed in astronauts. Previous studies performed with inclinations ranging from 0° to -15° have shown that a head-down tilt of -6° produces the best results for simulating weightlessness and is now generally acknowledged as standard [17].

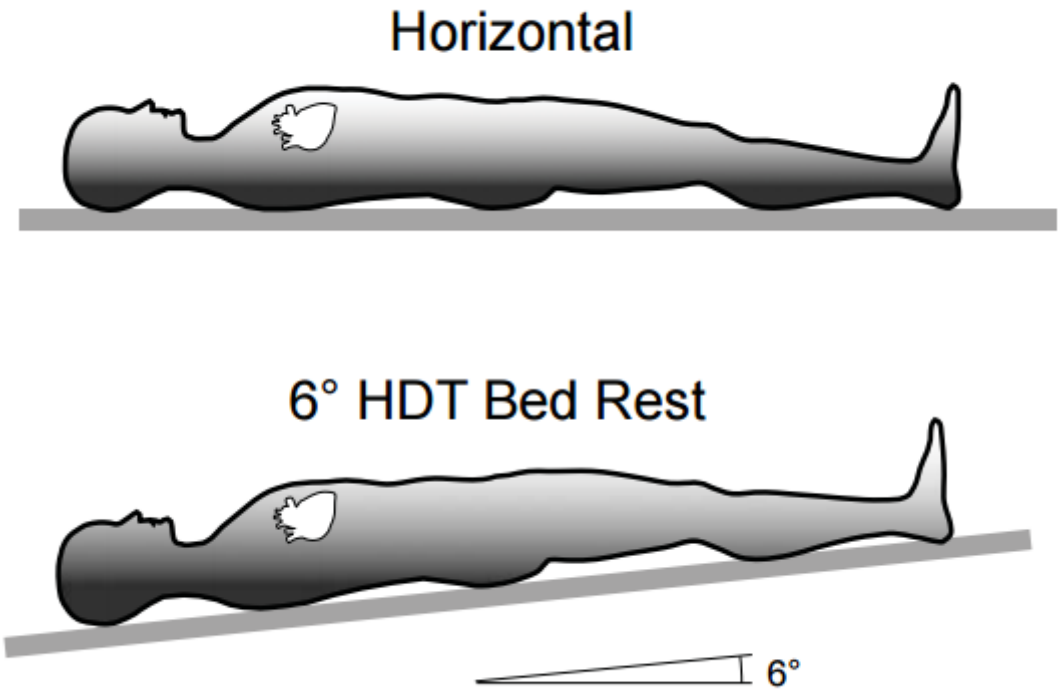

Fig. I.3: Tilting the bed head-down by 6° simulates the cephalic fluid shift observed in astronauts
Obtained from https://ispyphysiology.files.wordpress.com/2016/03/bed-rest.png

The HDBR studies performed by ESA are held in two clinical research facilities in Europe. The Institute for Space Medicine and Physiology (MEDES) based in Toulouse, France and the Institute of Aerospace Medicine as part of the German Aerospace Center (DLR) in

Cologne, Germany. HDBR campaigns are typically accompanied by an ambulatory period prior to bedrest and a post bedrest recovery period. The ambulatory period, during which normal physical activity should be maintained, serves for acclimatization and baseline data collection. The post bedrest period serves for the subjects to recover from the adverse effects of immobilization by physical exercise and for data collection during the recovery process. Of course, during the whole duration of bedrest, data is collected at appropriate intervals depending on the type of measurements taken.

Studies performed by ESA typically have one of the following study durations [17]:

- Short-term bedrest lasts for about a week with a minimum five-day ambulatory period. The rehabilitation period is depending on the study.
- Mid-term bedrest lasts for about three weeks with a 7-14 day ambulatory period and a recovery period of the same length.
- Long-term bedrest lasts for 60+ days and the ambulatory and recovery period each take at least 14 days.

Table 1: Selection of ESA bedrest studies performed.
Obtained from http://esamultimedia.esa.int/multimedia/publications/Bedrest_Resting_for_science

Name	Year	Location	Pre-bedrest days	Bedrest days	Post-bedrest days	Study	Angle
LTBR	2001–2002	Toulouse (FR)	15	90	15	Flywheel exercise Bisphosphonate	−6°
STBR	2001–2002	Cologne (DE)	9	14	3	Caloric variations in nutrition, Amino acid infusion	−6°
BBR	2003–2004	Berlin (DE)	3	56	6	Vibration exercise	0°
WISE	2005	Toulouse (FR)	20	60	20	Combined resistive exercise, aerobic exercise, lower body negative pressure Nutritional supplement	−6°
BBR2	2007–2008	Berlin (DE)	9	60	7	Testing resistive vibration exercise	−6°
BRAG1	2010	Toulouse (FR)	5	5	5	Artificial gravity by short-arm centrifuge	−6°
NUC	2010	Cologne (DE)	7	21	6	Testing nutritional supplement	−6°
BRAG2	2010–2011	Cologne (DE)	5	5	5	Testing an exercise protocol for use on a short-arm centrifuge	−6°
MEP	2011–2012	Cologne (DE)	7	21	7	Nutritional supplement	−6°

Throughout the HDBR campaign participants have to undergo various diagnostic tests and examinations, such as osteodensitometry, MRI scans, posturography tests, physical and mental stress tests or muscle biopsy and they have to donate blood and urine samples for

analysis. They have to follow a strict schedule and may have to regularly perform one or a combination of tasks of the afore-mentioned countermeasures.
All daily routines like showering, getting dressed and eating have to be done lying in bed as the participants are not allowed to even shortly sit or stand up during bedrest. There is some free time as well, but since some experiments may involve the mental aspects of isolation during spaceflight, contact to the outside world may be severely limited.

I.2 Mechanisms of vascular response

One of the major adverse effects of long term immobilization is a remodeling of the cardiovascular system and resulting orthostatic intolerance. This affects not only astronauts returning from long missions in space, but also numerous hospitalized patients on earth. It is therefore obligatory to understand underlying mechanisms, which control and regulate vascular response.

I.2.1 Vascular autoregulation

In every vascular network, blood flow is dependent on the tone of the vessel. This tone is maintained by isometric contraction of the vessel's smooth muscle cells and opposes the force exerted by the blood pressure. Under normal circumstances the vessel is always subject to a certain amount of tension. This tension is the product of two factors: the vessel's basal tone and a neurogenic tone [19].
The basal tone is mediated through local influences, usually originating in the vessel's wall itself or adjacent structures [20].
The neurogenic tone is mediated through sympathetic nerves running along between the vessel's adventitia and media. The neural network usually has the highest density in precapillary arterioles and is less dense in the venous, postcapillary system.
In organs, that are subject to a highly changing demand in blood supply, (e.g. skeletal muscles) the neurogenic tone is the main influence to blood flow.
The brain on the other hand has a very high but also very constant need for oxygen and nutrients. In such organs, the vessel's tension, and thus the blood flow, is primarily modulated via the basal tone.
Endocrine agents circulating in the bloodstream can further influence the state of the vessels.

I.2.1.1 Central influences on vascular tone

Almost all vascular networks (the only exception being the placenta and the umbilical cord) are influenced by the autonomic nervous system (ANS). Sympathetic nerves play the major role in this autonomous innervation. Depending on the type of receptor activated by the sympathetic neurotransmitter noradrenaline (NA), different reactions can be achieved. The prevalent types of adrenergic receptors are the G-protein-coupled α_1- and the β_2-receptors.

α_1-adrenergic receptors trigger a cascade (phospholipase C → inositol triphosphate) that will lead to an increase in Ca^{2+}-concentration. This causes smooth muscle cells to contract, leading to vasoconstriction.

β_2-adrenergic receptors trigger a cascade (adenylate cyclase → cAMP) that will lead to a decrease in Ca^{2+}-concentration, ultimately leading to vasodilation [21].

Another factor influencing blood vessel regulation on a systemic level are circulating hormones like adrenaline and NA as well as angiotensin II. Blood vessels have α- and β-receptors also responding to the blood borne catecholamines adrenaline and NA. The effect of vasoconstriction or –dilation depends on the concentration of the receptor type in the affected organ.

Angiotensin II is the main vasoactive agent of the renin-angiotensin-aldosterone-system and a potent vasoconstrictor [21, 22].

I.2.1.2 Local influences on vascular tone

The concentration of certain metabolic factors within a vascularized region controls blood flow on a local level. An increase in pCO2, lactate or potassium, and a decrease in pO2 or pH will cause vasodilation. This leads to increased blood flow in metabolically active regions [21].

Another way to control local blood flow is the Bayliss-effect, a myogenic response to a change in blood pressure. With increasing pressure the vessel's smooth muscle cells are stretched. They will respond by contracting, which will increase the vessels resistance [23]. Figure I.4 shows how this effect is used to maintain a steady blood flow despite sudden changes in blood pressure.

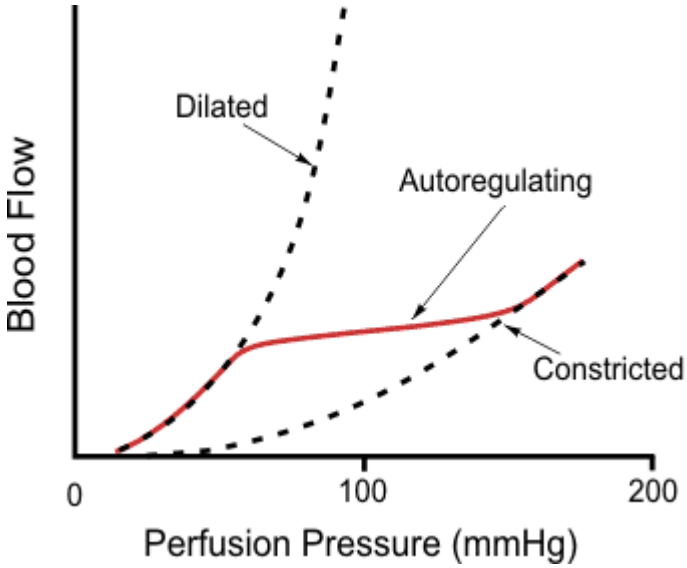

Fig. I.4: The Bayliss-effect keeps blood flow constant over a wide range of pressures.
Obtained from http://www.cvphysiology.com/Blood%20Flow/bf004_autoregulation_curve.gif

I.2.1.3 Endothelial modulation of vascular function

The endothelium plays a major role in vascular autoregulation by producing and releasing as well as activating and deactivating vasoactive agents [24]. Figure I.5 shows an overview of the most important endothelial functions regulating vascular tension.

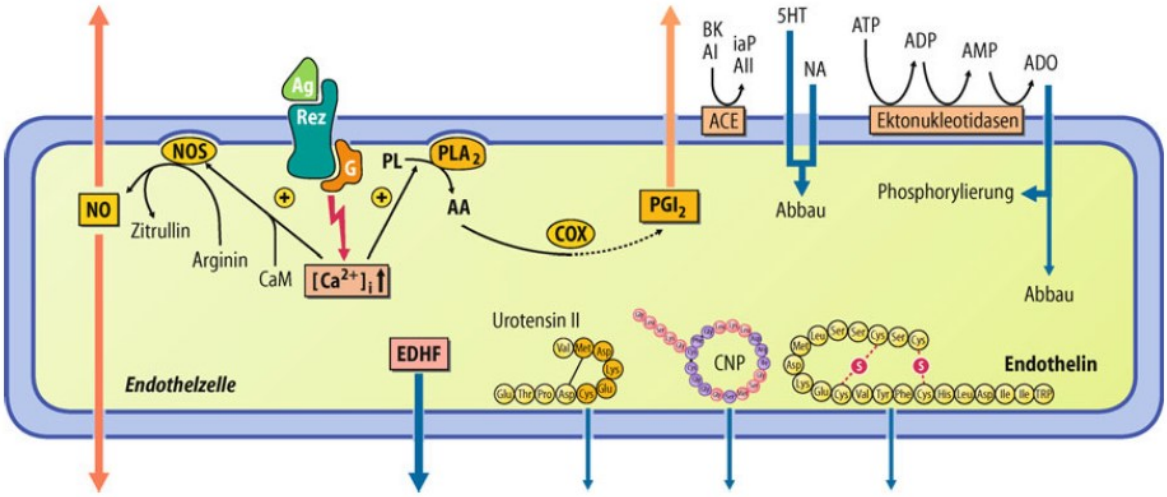

Fig. I.5: The main vasoactive reactions in an endothelial cell.
Obtained from Schmidt, Lang; Physiologie des Menschen; S.601

The most prominent vasoactive agent produced in the endothelial cell is nitric oxide (NO), sometimes referred to as endothelium-derived relaxing factor (EDRF). NO is produced by endothelial NO-synthases (eNOS) as a response to increased intracellular Ca^{2+}-concentration, caused by vascular shear stress or binding of certain agents like bradykinin,

histamine or acetylcholine. By activating guanylyl cyclase in smooth muscle cells, NO causes an increase in cyclic guanine monophosphate (cGMP), leading to relaxation of the smooth muscle and thus vasodilation. Many of the agents, which activate the eNOS are themselves vasoconstrictors. NO-triggered vasodilation counteracts this constriction, making the vascular response the net result of the two effects [19, 25].
Exogenous NOs have the same vasodilatory effect and are used as an emergency medication in case of acute angina pectoris or heart attack.
Prostacyclin (PGI_2) follows a very similar pathway, also increasing cGMP in smooth muscle cells and thus causing vasodilation [26]. Endothelium-derived hyperpolarizing factor (EDHF) is another vasodilator expressed mainly in small vessels and when NO production is reduced [27].
Endothelin and Urotensin, on the other hand, are vasoconstrictors. They play only a minor role in regulating changes in blood pressure, but rather help maintaining the vessel's basal tone.

I.3 Assessing vascular function via retinal vessels

Vascular autoregulation and dysfunctions therein are important factors in common diseases like arthrosclerosis, hypertension or coronary heart disease. When trying to understand vascular function it is important to measure vascular response. The gold standard for assessing vascular function is flow mediated dilation (FMD). Arteries respond with dilation when blood flow through them is increased. The main factor for this dilation is the release of endothelial NO due to shear stresses caused by the increased flow [28]. FMD assessment involves depicting an artery (usually the brachial artery) with ultrasound and placing a cuff distal of the ultrasound probe. Inflating the cuff inhibits blood flow in the artery. Releasing the cuff after a period of inhibited perfusion induces reactive hyperemia and thus increases blood flow, which will lead to dilation of the vessel. The ultrasound images are used to calculate the artery's diameter during this procedure.

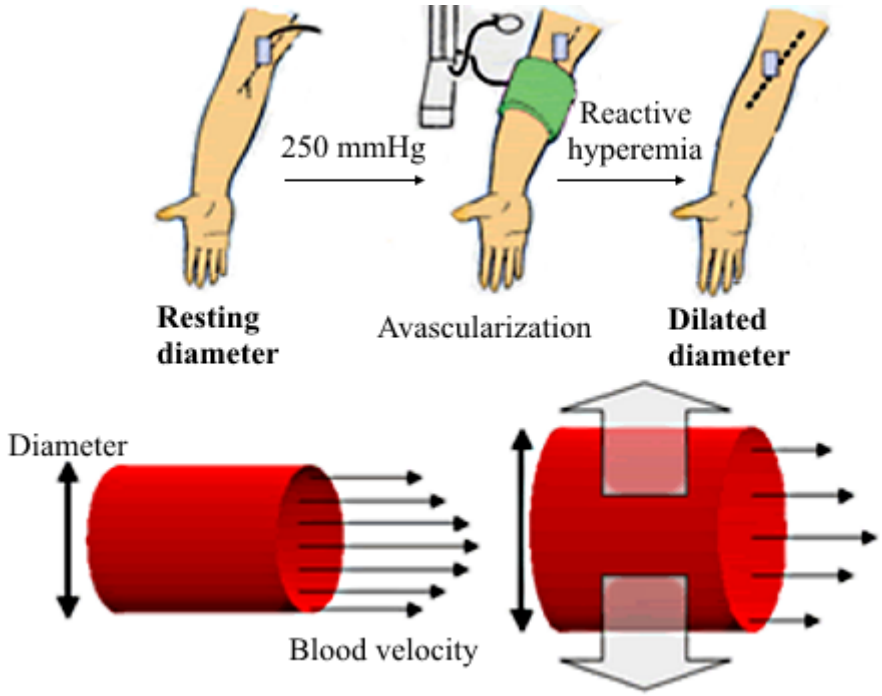

Fig. I.6: Flow mediated dilation induces reactive hyperemia to measure the vascular response to increased blood flow
Image modified from http://hivandhepatitis.com/legacysite/0_2010_images/flow_mediat.gif

FMD measurements can be very time-consuming and tedious, as the ultrasound probe needs to be positioned precisely and the subject must not move during the whole procedure. They require a lot of experience and results often vary with protocol or operator [29].

Because of its unique accessibility, the retinal vascular network offers a much easier way to measure vascular response through retinal imaging. The eye's vascular network allows a quick, non-invasive and reproducible way to assess vascular function and detect early signs of vascular dysfunction [30, 31].

I.3.1 Structure of the human eye

The human eye, as basically the eye of any vertebrate, is a lensed eye, meaning it uses a lens to focus incoming light on the receptive cells. This allows for a sharp and at the same time bright image perceived.
In primitive organisms the sensing of light happens through photoreceptive cells located at the surface of the organism, so-called eyespots. While those eyespots make it possible to discern brightness, they are only able to detect the direction of incoming light on a very

rudimentary level. Invagination of the eyespot greatly improves the discrimination of direction, because depending on the angle of incoming light, only certain receptive cells are activated. However, increasing the depth of this “eye-cup” can only improve the organism’s eyesight to a certain extend. By narrowing the aperture of the pit, a sharper perception becomes possible. The underlying mechanism resembles that of a pinhole camera. Through the narrow opening only a small amount of light coming from a given direction can hit receptive cells corresponding to that direction. This results in a higher spatial resolution, which can be further improved by increasing the number of receptive cells. The downside of the pinhole aperture is that altogether a smaller amount of light can enter the eye, resulting in a darker image. The evolution of the lensed eye mitigates this problem. The lens can focus incoming light on a small spot on the layer of photoreceptors while keeping the overall aperture of the eye big enough for a lot of light to pass through. This results in a high resolution image and at the same time a high sensitivity to light [32].

I.3.1.1 Location and musculature

The eye is a twin organ located in a pyramidal socket in the skull called the orbit. Its shape resembles a sphere with an average diameter of about 24 mm and a weight of roughly 7.5 grams [33].

Six external or extraocular muscles control the movement of the eye within three degrees of freedom. Three cranial nerves (N. oculomotorius, N. trochlearis, N. abducens) control the horizontal and vertical rotation of the eye [34]. Although possible, rotation around the sagittal axis cannot be controlled voluntarily.

At the back of the socket there is fatty tissue cushioning the eyeball and keeping it in place. The optic nerve, carrying the visual signal to the brain, exits the orbit thorough the optic canal [35].

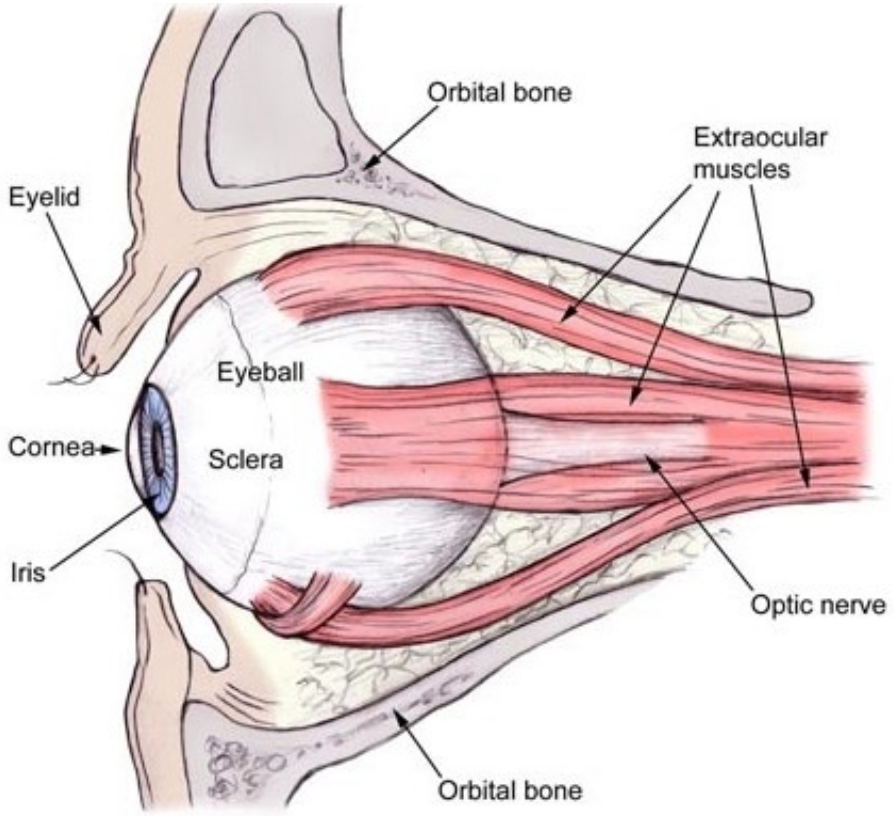

Fig. I.7: Location of eyeball and extraocular muscles in orbit
Obtained from http://1.bp.blogspot.com/-g9bLiTCoJC0/ThuZuZ3vr5I/AAAAAAAAAAo/IF4Sza8rTQM/s1600/the+eye+orbit.jpg

I.3.1.2 Layering of the eyeball

The human eye can be differentiated in a front and a back part. The front part is roughly 7 mm in length and contains most of the optical apparatus. The back part of the eye is mainly formed by the eyeball's wall and the vitreous chamber [33].

The eyeball's wall consists of three distinct layers: the sclera, the choroid and the retina. The sclera is the outermost shell of the eyeball. It is made up of connective tissue, blood vessels and nerve fibers. Its main purpose is to give the eye its form and rigidity and it is the insertion point of the extraocular muscles. In the front of the eye, the sclera turns into the cornea. The cornea's curvature is bigger than that of the sclera, which makes it stand out of the rest of the eyeball. The bigger curvature is also important as it forms the eye's anterior chamber. The cornea's arrangement of connective tissue, its missing vascularization and the unmyelinated nerve fibers make the cornea translucent. This is essential as light needs to be able to shine through it. Both the sclera and the cornea together are called the fibrous tunic [36].

Moving inward, the next layer is the choroid. It is strongly vascularized to provide enough blood flow to the outer layer of photoreceptor cells. The choroid also contains the pigment

melanin to prevent scattering of the incoming light. In the front of the eye, next to the choroid, there is the ciliary body containing the ciliary muscle. The lens is held in place by zonular fibers connecting it to the ciliary body. By contraction or relaxation of the ciliary muscle, these fibers loosen or tighten and thus the flattening of the lens changes. This changes the refractive properties of the lens, a process called accommodation, which is used to perceive objects at different distances. In front of the ciliary body lies the iris, which forms the main aperture of the eye called the pupil. By changing its width and thus changing the diameter of the pupil, the iris can regulate the amount of light entering the eye. The choroid, the ciliary body and the iris together are called the uvea or the vascular tunic.

The innermost layer of the eyeball is the retina. It contains different types of neurons responsible for detecting light and generating and forwarding neural signals. There are also some inhibiting neurons as well as glial cells, responsible for structural integrity and nourishment of the neurons. The retina also possesses a system of blood vessels, which will be of great importance for this subject and will be discussed more in depth later on.

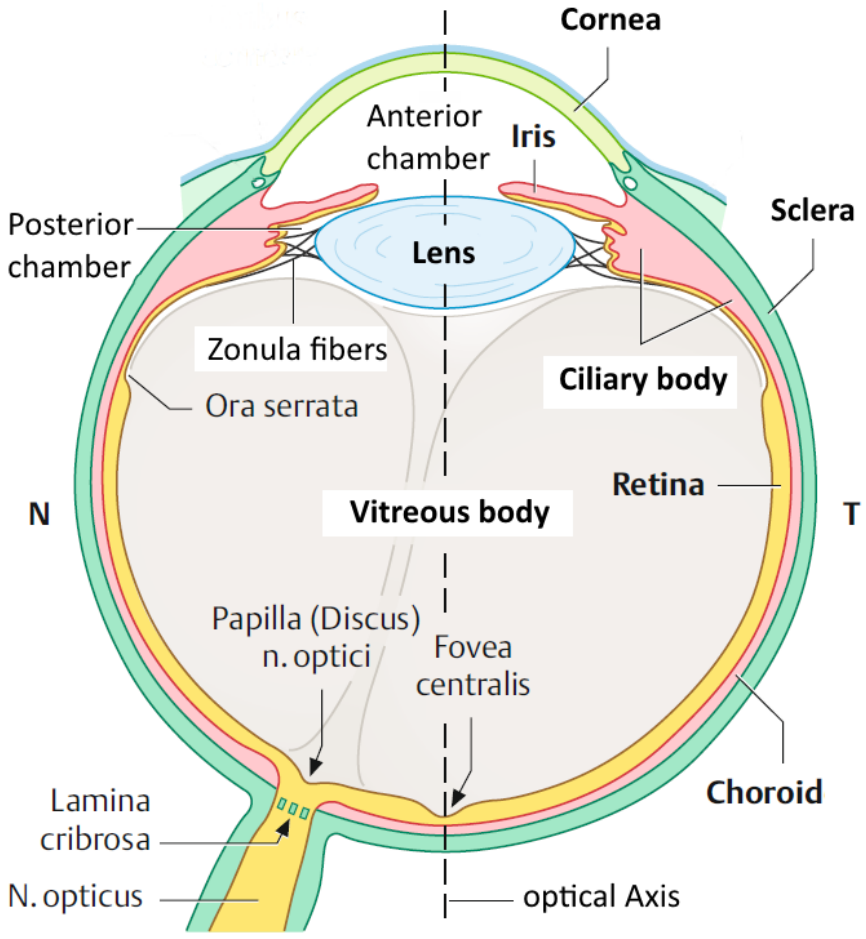

Fig. I.8: Cross section of the eyeball.
N nasal, **T** temporal, **green** fibrous tunic**, red** vascular tunic, **yellow** retina
Modified from Lüllmann-Rauch; Histologie; S.633

I.3.1.3 The optical apparatus

For an image to be perceived, light has to travel from an object to the retina. On its way the light has to traverse the optical apparatus of the eye. The rules of optics apply and the image created on the retina is an inverted, scaled-down image of reality. The optical apparatus consists of the cornea, the anterior chamber, the lens and the vitreous body. Each of these structures adds to the total refractivity of the eye.

I.3.1.4 Histology of the retina

The retina is the innermost, light sensing layer of the eye. It is divided into two parts separated by the ora serrata: the blind part (pars caeca) consists only of a pigmented layer (stratum pigmentosum) and covers the backside of the iris and the ciliary body. The visual part (pars optica) consists of an outside pigmented layer and an inside nerval layer (stratum nervosum).

The pigmented layer (Fig.I.8 1=PE) is a single-layered epithelium and builds the connection between retina and choroid (Fig.I.8 ChK). This epithelial layer, called stratum epithelium, is not adnate to the retina but has only an adherent connection, making a retinal detachment possible.

The nerval layer abuts the pigmented layer on the inside and has a width of about 0.2 mm. It contains the first three neurons of the visual pathway: the photoreceptive cells, the bipolar cells and the retinal ganglion cells. Histologically, the retina is subdivided into ten layers (Fig.I.8 1-10). The neurons' nuclei are in layer 4, 6 and 8.

The outermost layer of neural cells are the photoreceptive cells (1st neurons): rod cells for detecting the intensity of light and thus discerning light from dark (scotopic vision) and cone cells for detecting different wavelengths of light and thus discerning color (photopic vision). There are about 120 million rod cells and 6 million cone cells [33, 37].

The bipolar cells (2nd neurons) receive the signal coming from the photoreceptive cells and forward it to the third neurons.

The ganglion cells (3rd neurons) build the innermost layer of the retina. Their axons converge at the optic disc where they form the optic nerve and leave the eyeball trough a mesh in the scleral tissue called the lamina cribrosa. There are about one million ganglion cells conveying the signal of a total of 126 million rod and cone cells.

Since the photoreceptive cells are the outermost part of the pars optica, the light has to permeate the layers of ganglion and bipolar cells to reach and stimulate the photoreceptors.

This structural design has evolutionary and embryological reasons and is called an inverse retina [36].

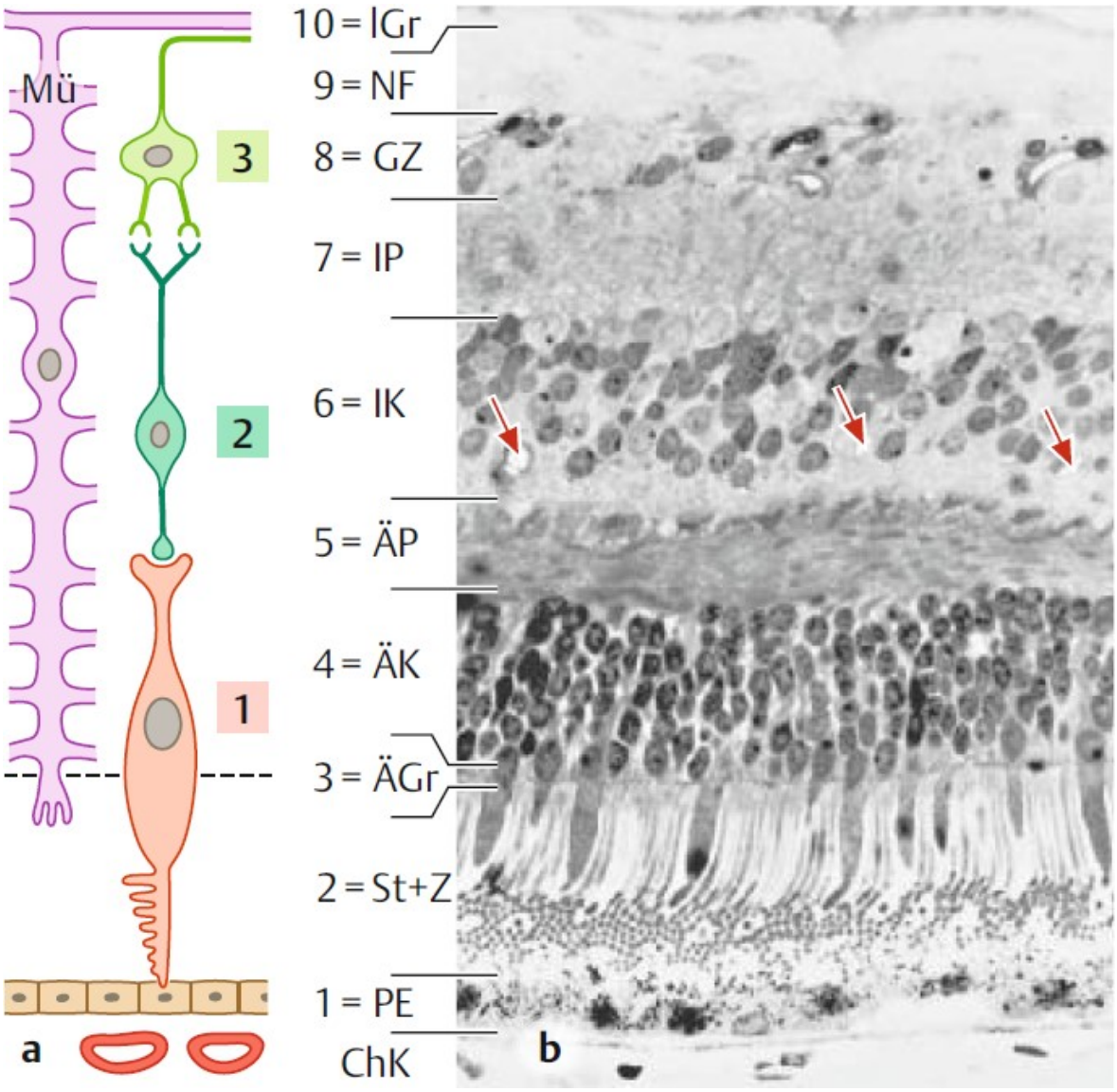

Fig. I.9: Histological layers of the eyeball.
a Schematic drawing showing the three neurons, **b** Histological section
Arrows pointing to vessels emanating from the central retinal artery
Obtained from Lüllmann-Rauch; Histologie; S.650

I.3.2 The fundus

The back of the eye visible when examining a patient's eye with an ophthalmoscope is called the fundus. It is orange to red in color, which stems from the blood-rich choroid shining through the retina. Important structures discernable on the fundus are the macula lutea, the optic disc and the central retinal vessels.

The macula lutea (yellow spot), or simplified just macula, is at the center of a standard funduscopic image. It is where the optical axis meets the retina, slightly temporal of the bulbus' geometrical axis. The macula has a diameter of about 3 mm. At its center is an indentation called the fovea centralis. This indentation stems from the inner retinal layers (i.e. the bipolar and ganglion cells) being translocated towards the outer regions of the fovea. Thus light will not be scattered when it hits the foveal photoreceptors, which in this region consist almost solely of cone cells. Their density at the center of the fovea, called the foveola, is about 150.000/mm² and decreases quickly to about 5.000/mm² at the periphery of the retina [37]. The large number of cone cells and the unhindered passage of light make the fovea the area of the highest spatial resolution and thus the sharpest vision. The fovea has a diameter of about 1.4 mm and its surrounding area is called the parafovea and, moving further out, the perifovea.

Only about five millimeters nasal of the area of sharpest vision is the optic disc, the so-called blind spot. It is where the ganglions' axons are bundled together to exit the eye as the optic nerve. At the area of exit there are no receptive cells and thus no visual perception is possible at the optic disc, hence the term blind spot. The diameter of the optic disc lies between 1.8 and 1.9 mm [38]. At the same site where the optic nerve exits the eye, the central retinal vessels enter it [39].

Figure I.10 shows a funduscopic image of the right eye, depicting the most prominent structures of the fundus, the macula, the blind spot and branches of the central retinal vessels.

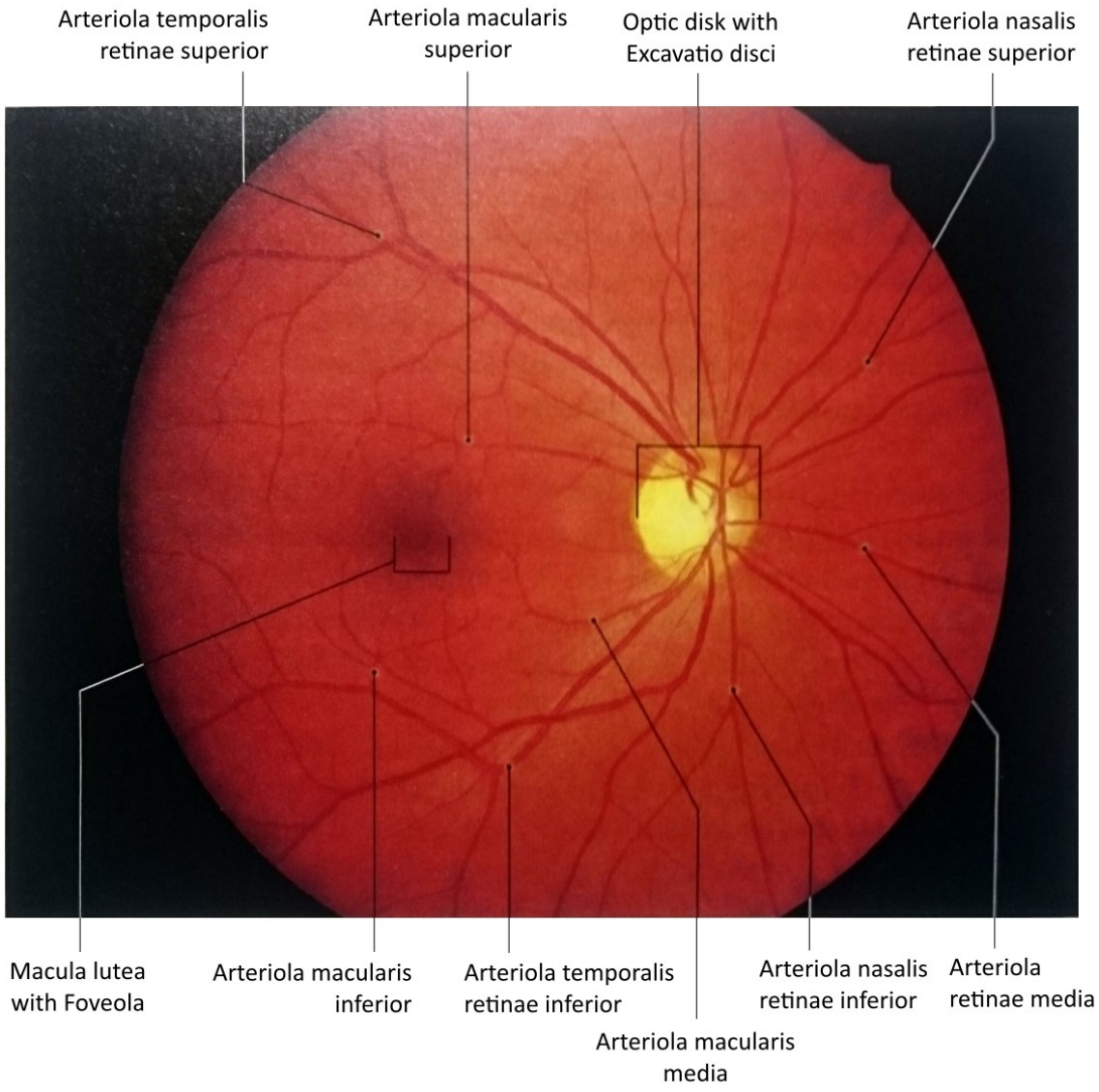

Fig. I.10: Fundoscopic image showing the fundus' structures.
Modified from Zilles, Anatomie, S.670

I.3.3 Central retinal vessels

The photoreceptors are a metabolically highly active tissue. To ensure sufficient blood flow, two vascular structures nourish the retina. The choroid supplies the outside of the retina while the central retinal artery and its branches supply the retina from the inside. As mentioned earlier, the optic disc is where the blood vessels enter the eye. At the disc's center is a small pit, the excavatio disci, from where the central retinal artery (CRA) and central retinal vein (CRV) spread out to vascularize the inner layer of the retina. The CRA is the first branch of the ophthalmic artery, which again is a branch of the internal carotid artery. The central retinal artery enters the optic nerve and follows its course for about a

centimeter before it enters the eyeball. Outside the sclera it is called the extraocular part, having passed the lamina cribrosa it is named the intraocular part [35].
Upon leaving the optic nerve at the center of the optic disc, the CRA and CRV spread out radially. They form four main branches, one for each retinal quadrant. Smaller branches vascularize the areas in between the quadrants and the macula lutea [34].

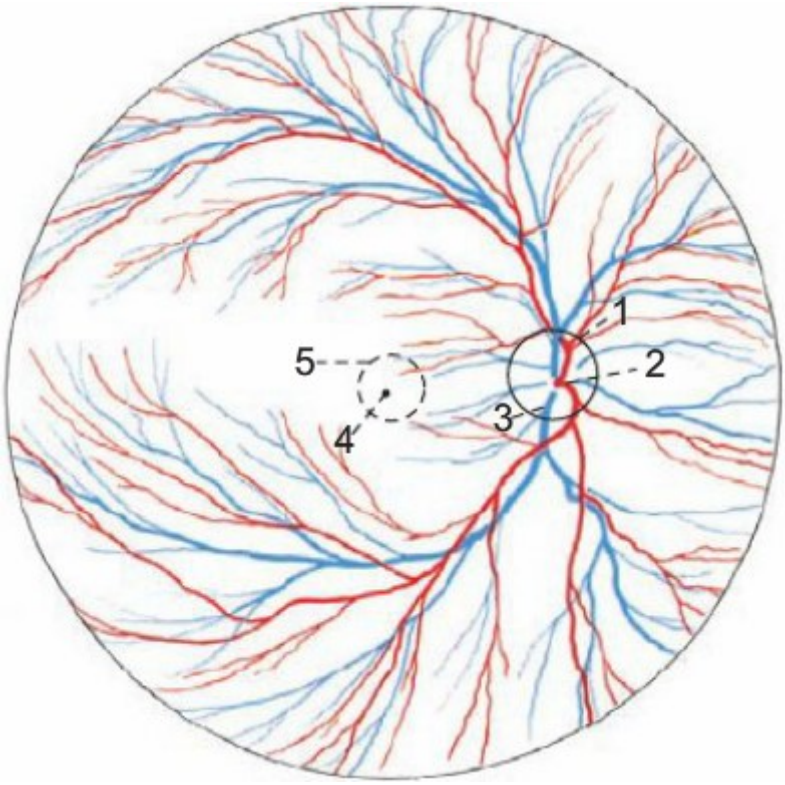

Fig. I.11: Schematic view of the central retinal vessels
1 Optic disc, **2** CRA, **3** CRV, **4** Fovea centralis, **5** Macula lutea
Obtained from Trepel; Neuroanatomie; S.324

I.3.3.1 Development of central retinal vessels

In the early stages of the eye's embryological development the retina is nourished by the hyaloid vasculature. The central retinal vessels emanate from the optic disc to grow a vascular network for the inner layers of the retina. In the beginning of this network's development astrocytes bud out and cover the retina's inner surface [40, 41]. They migrate towards the periphery leaving out the area around fovea, which will remain void of blood vessels. The relative hypoxia in the still avascular retina triggers the expression of vascular endothelial growth factor (VEGF) within the astrocytes [41]. VEGF is the main stimulus for angiogenesis and causes endothelial cells to proliferate. As those endothelial cells develop into fully fledged blood vessels the hypoxia is reduced, decreasing the astrocytes'

expression of VEGF. The process of angiogenesis follows this gradient of VEGF and stretches out towards the periphery. The exact location of vessels to form depends on the mesh grown by the astrocytes and presumably other factors still to uncover. The result is a pattern of central retinal vessels so unique it can be used to identify a person biometrically [42]. The oxygen supplied by this network of blood vessels will cause apoptosis and differentiation in the astrocytes, terminating their expression of VEGF [43]. At the same time as the network of retinal vascularization grows, the hyaloid vasculature regresses. In the end the inner retina is supplied only by the central retinal vessels stretching from the optic disc to the periphery.

Ebryologically the eye develops as an extension of the diencephalon. This close relation results in a comparable development of blood vessels in the brain and the eye and consecutively in similarities in cerebral and ocular vascularization. In both organs a dense network of capillaries perfuses a metabolically highly active region. In both capillary structures endothelial cells form a barrier, controlling the nutrient exchange and buffering changes in the blood's composition. These similarities make the eye's blood vessels a good model for cerebral vasculature and make it possible to better understand changes in the brain's microcirculation by looking at the eye.

I.3.4 Retinal imaging

Since the eye's structures need to be translucent in order to fulfill their purpose, the eye offers the unique opportunity to observe the microcirculation non-invasively and repeatedly. Funduscopy, or ophthalmoscopy, is used to inspect the retina in real-time and is part of a routine ophthalmological examination. In retinal imaging, technical equipment is used to capture an image of the retina. There are several ways to visualize and capture images of the retinal structures. The most common one is classical fundus photography.

In fundus photography a specialized camera is used to take a color image of the fundus. Light is emitted from the camera, passed through the pupil and reflected by the retina. The reflected light is passed through the camera's lens system and captured by a digital image sensor. The resulting image is a 2D representation of the retinal structures (cf. Fig. I.10). Different color filters or special dyes may be applied when taking the picture. To achieve a satisfying image, it may be necessary to dilate the pupil with mydriatic eye drops. Modern fundus cameras use infrared light, eliminating the need for pupil dilation.

The image taken by the fundus camera can be saved for later reference or software analysis.

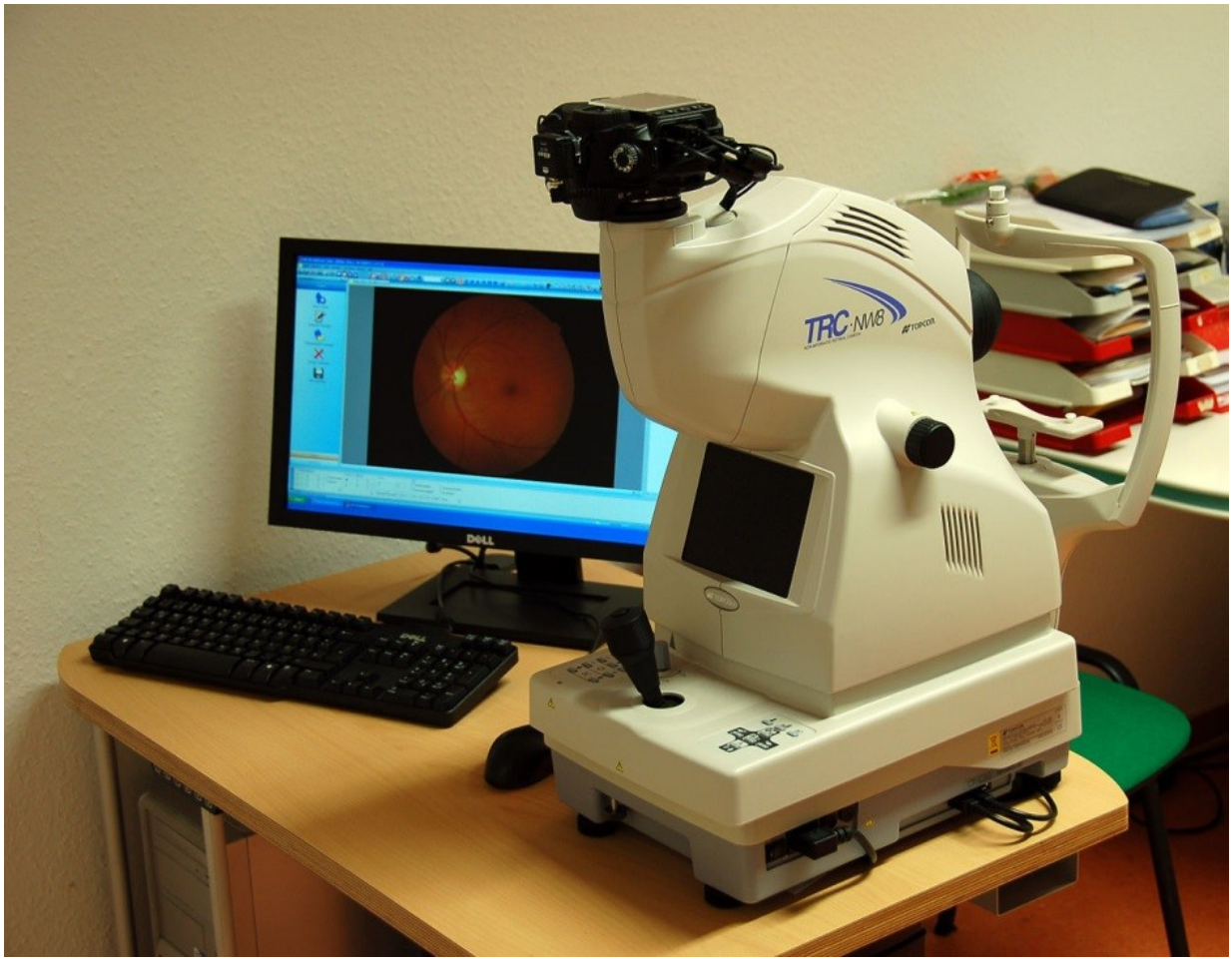

Fig. I.12: A tabletop fundus camera

Note the relative size of the lens and control system compared to the camera on top.

Obtained from https://upload.wikimedia.org/wikipedia/commons/thumb/7/73/2010-12-07-funduskamera-by-RalfR-02.jpg/1280px-2010-12-07-funduskamera-by-RalfR-02.jpg

II. AIMS AND OJECTIVES

Changes in vascular function are a problem often observed in astronauts as well as people undergoing long term bedrest. Vascular dysfunction is an important factor in the pathogenesis of common diseases such as hypertension, atherosclerosis or diabetes. The retina offers a unique opportunity to study the microcirculation and changes within it in vivo, repeatedly and non-invasively. Because of their close relation concerning development and functionality, observing changes in central retinal microvasculature may as well help to gain a better understanding of processes in the cerebral or coronary microcirculation. Spaceflight has also shown to influence astronauts' eyesight, leading to sometimes irreversible degradation in vision. Studying the eye during simulated microgravity might help to understand changes in vision happening during spaceflight.

The aim of this diploma thesis is to assess microvascular changes in patients undergoing long term 6° head-down bedrest. This is done by imaging the central retinal vessels with a non-mydriatic, handheld fundoscopic camera and analyzing the calculated arterial and venous diameters as well as arterio-venous ratios. It will also be possible to further evaluate retinal imaging as a means of studying vascular function and changes therein.

It was hypothesized that the retinal vessels' diameter, especially arterial diameter, will decrease within the first days of bedrest in response to cephalic fluid shift and increased hydrostatic pressure. After a couple of days of bedrest however the cardiovascular system is expected to adapt to changed conditions and retinal vessel diameter will normalize.

III. METHODOLOGY

III.1 MEDES space clinic

The study was carried out by MEDES, the French Institute for Space Medicine and Physiology. It was conducted at the MEDES Space Clinic, a clinical research center on the site of Rangueil University Hospital in Toulouse, France. Commissioned in 1996, the Space Clinic offers controlled environmental conditions such as temperature, light and acoustics regulation, and various laboratories and equipment for research. Six rooms with two medical beds each offer room for twelve subjects [44].

III.2 Subjects

Data was collected from a total of ten subjects.

III.2.1 Subject selection

The subjects were selected from a range of volunteers recruited by MEDES. Prior to inclusion they underwent a clinical examination comprised of:

- Blood pressure measurement in supine position
- ECG
- Osteodensitometry
- Tilt table test
- Blood test: hematology, liver and kidney function, metabolical, hormone and vitamin status and virology (hepatitis, HIV)
- Genetic testing for factor V Leiden thrombophilia
- Urine test (glucose, bilirubin, ketone body, blood, protein, urobilinogen, nitrite, leukocytes)
- Toxin screening of urine (nicotine, cannabis, barbiturates, benzodiazepines, opiates) and blood (alcohol)
- Pulmonary radiography (front and side view)
- Cycling ergometer (VO_2 max)
- Lower limb Doppler sonography

III.2.1.1 Inclusion criteria

- Healthy male adult
- Age between 20 and 45 years

- Body size between 1.58m and 1.90m
- Body mass index (BMI) between 22 and 27
- Non-smoker
- Currently covered by a social security system
- Signed consent form
- No other engagements during the time of the study

III.2.1.2 Exclusion criteria

- Regular intake of medication or nutritional supplements
- Pathologic results on any of the tests mentioned in III.2.1
- History of thyroid dysfunction, kidney stones, diabetes or migraine
- Personal history or family record of thrombosis or thrombophlebitis
- Personal history or family record of psychological disorders
- Personal history or family record of obesity or type 2 diabetes
- Past or present claustrophobia
- Color blindness
- Metallic implants or osteosynthesis material
- Addiction to alcohol, drugs or video games
- Participation in another clinical research study

III.2.1.3 Dropout criteria

- Recent illness or disease
- Upon subject's request

III.2.2 Ethical considerations

This study was evaluated and approved by the ethics committee at MEDES. Written informed consent was obtained from every volunteer.

III.3 Study design

This study was performed as part of an ESA long-term bedrest (LTBR) study. LTBR studies are performed on a regular basis to simulate physiological changes observed during spaceflight, including:

- Changes in the cardio-circulatory system, blood pressure and heart rate control
- Decrease in muscle mass and altered neuronal control

- Loss of bone density, especially in weight-supporting bones
- Changes in posture and locomotion control
- Altered nutrient absorption and control of excretion of salt and water
- Development of glucose intolerance and insulin resistance

Almost all of these changes reported in spaceflight have also been observed in bedrest studies [17, 45, 46]. One objective of bedrest studies is to gain a deeper understanding of the regulation mechanisms happening during HDBR.

Another objective is to develop and test countermeasures to mitigate those changes. Possible countermeasures include both resistive and vibration exercise, alteration in fluid distribution by application of lower body negative pressure or centrifugal force (artificial gravity), and different nutritional cocktails, infusions or medication.

Bedrest campaigns are further useful for developing and improving methods and biomedical equipment for monitoring and diagnostics, like portable devices to continuously and non-invasively monitor cardio-circulatory parameters or innovative techniques to measure the electrical activity of the muscles.

Fig. III.1: A volunteer undergoing head down tilt bedrest
Image courtesy of ESA (www.esa.int)

This study was part of ESA's LTBR-Cocktail study, the aim of which was to evaluate the effects of a Cocktail-dubbed countermeasure on adaptation mechanisms during 60 days head-down tilt bedrest.

A total of twenty subjects were recruited into two groups of ten subjects, the “cocktail” or intervention group and the control group. They underwent bedrest in two campaigns, each with ten subjects randomly chosen out of the two groups. Each campaign lasted for a total of 88 days: 14 days of pre-bedrest (days -14 to -1), 60 days of HDBR (days 1 to 60) and 14 days of recovery (days +0 to +13). Additional examinations were performed on day +30 (1 month), day +360 (1 year) and day +720 (2 years).
The intervention group received a daily dose of 741mg of polyphenols, 168mg of vitamin E mixed with 80µg selenium and 2.1g of omega-3-acid. The control group did not receive any medication. The study was conducted as a double-blind study with the cocktail being administered together with the food. Neither subjects themselves nor investigators knew which group a subject belonged to.
The data presented in this diploma thesis was collected during the first LTBR-Cocktail campaign.

III.4 Data collection

Retinal images were obtained five times during pre-bedrest (baseline data collection, BDC) and bedrest (head down tilt, HDT) periods. Table 2 shows the exact days the retinal imaging was done.

Table 2: Data collection timeline

	Pre-bedrest	**Bedrest**			
Study day	-2	1	8	16	29
Time point	BDC-2	HDT01	HDT08	HDT16	HDT29

III.4.1 Fundus camera used for obtaining images

Retinal images were obtained using a lightweight handheld fundus camera. Conventional fundus cameras usually have to be placed on a table top (cf. Fig.I.11) and are not suitable for examining patients lying in bed.
The device used for obtaining the images was the Smartscope Pro fundus camera with the Retinal module EY4 objective (Optomed Oy (Ltd.), Oulu, Finland) for non-mydriatic fundus imaging.

Fig. III.2: The Smartscope Pro retinal imaging camera
Modified from
https://static.wixstatic.com/media/fe6c61_e1799bdbda374308bec00a4eefcd52b1~mv2_d_2612_2470_s_4_2.png

When looking into the camera a small red dot can be seen in the field of view. Focusing on the dot centers different parts of the retina on the camera's image. The dot is moved by the camera's operator in order to center the retinal structure, which needs to be examined. For this study the optic disc had to be at the image's center so the dot was moved accordingly for each eye.

For BDC-images the subjects were in supine position on a level surface. For HDT-images they were in supine position on a bed tilted -6° head down. To obtain better image quality the room was darkened and a piece of cloth was placed over the subject's head and the fundus camera to block any remaining scattered light.

Fig. III.3: Example image of using the Smartscope Pro on a lying person.
Video still image obtained from https://youtu.be/EozNT5oaP30

Each time two pictures were taken per eye, resulting in 20 pictures per subject. The Smartscope Pro camera creates three JPEG-images per picture taken: a true color image, a grayscale image and a color-corrected (red filtered) image. After every fundus photographing the twelve resulting images (two pictures per eye, three images per picture) were saved on a computer and forwarded for image analysis.

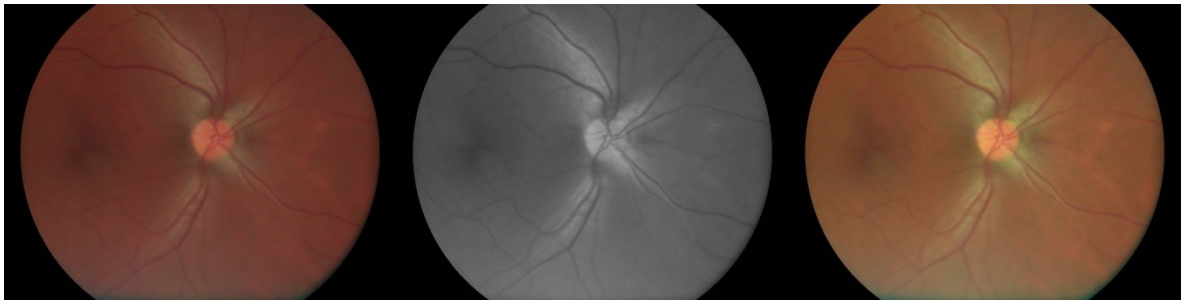

Fig. III.4: Comparison of the retinal images saved by the camera.
Left: true color, **Middle:** grayscale, **Right:** color-corrected

III.4.2 Image analysis

The retinal images were analyzed using the software iFlexis developed by VITO (Mol, Belgium). The true color images were used by the software to calculate the desired parameters. Because of early branching of the central retinal artery/vein these vessels' diameters cannot be measured directly but their equivalents have to be calculated from their branches.

Formulas developed by Parr et. al. and Hubbard et. al., and revised by Knudtson et. al. were used to calculate central retinal artery and vein equivalent (CRAE, CRVE) [47–49]. Retinal vessels were analyzed within a ring between half a disc diameter and one and a half disc diameters from the optic disc's rim. The six largest arteries and six largest veins inside the ring were chosen to perform calculations [49].

The average of both eyes was calculated for CRAE and CRVE per time point. From these averages arterio-venous ratio (AVR) was formed.

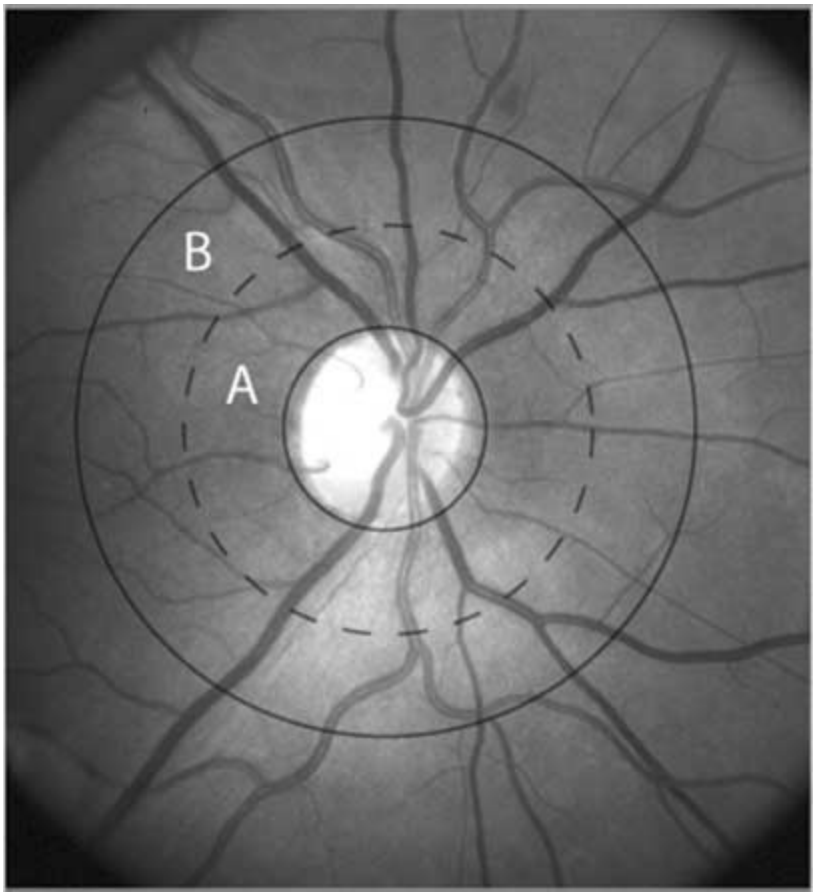

Fig. III.5: Retinal image's region of analysis
Region A is half a disc diameter from the optic disc margin
Region B is half a disc diameter to one and a half disc diameters from the margin
Retinal vessel diameter measurements were performed in region B
Image obtained from Knudtson et. al [49]

III.5 Statistical analysis

Values were calculated using Microsoft Excel 2010 (Microsoft Inc.) and are presented as averages ± standard deviation (SD). Paired t-test was used to calculate differences between sampling points. A p-value less than 0.05 was considered statistically significant.

$p < 0.05$ (*), $p < 0.01$ (**)

IV. RESULTS

All ten subjects successfully completed the LTBR-study. At each time point useable data could be gathered from the subjects for analysis.

All subjects were adult, healthy males between 20 and 45 years of age (average 34.2 years). They were between 1.68 m and 1.84 m tall (avg. 1.76 m) and weighed between 65 kg and 84.9 kg (avg. 73.5 kg). This results in BMI between 21.9 and 25.4 with an average BMI of 23.6.

Table 3: Anthropometric data of subjects. A-J represents the test subjects

Subjects	A	B	C	D	E	F	G	H	I	J
Age	41	29	20	42	36	45	25	24	39	41
Height [m]	1,74	1,84	1,84	1,69	1,81	1,75	1,81	1,72	1,68	1,76
Weight [kg]	67,3	74,5	74,0	65,0	84,9	75,3	83,2	69,0	70,7	70,4
BMI	22,2	22,0	21,9	22,8	25,9	24,6	25,4	23,3	25,0	22,7

IV.1 Central retinal artery equivalent

CRAE represents the mean diameter of the subjects' central retinal arteries. The mean CRAE was 128.78 ± 10.65 µm. Table 4 lists the subjects' values for each time point.

Table 4: CRAE of subjects (values in µm)

Time point	A	B	C	D	E	F	G	H	I	J
BDC-2	126,34	133,63	117,75	129,52	130,78	125,98	121,02	152,94	133,38	132,71
HDT01	127,75	125,72	118,70	132,20	133,68	120,41	123,00	153,96	138,61	141,14
HDT08	118,32	123,08	121,83	128,23	128,95	117,31	110,71	150,82	122,73	132,12
HDT16	123,15	130,36	129,44	132,62	139,48	119,27	108,72	153,88	130,45	130,47
HDT29	118,69	121,84	118,00	135,79	131,42	118,05	116,63	146,43	125,77	135,37

The data show an overall decrease in CRAE during bedrest with a net difference of 3.6 µm between baseline data collection and the last day of measurement. Statistically significant drops in arterial diameter occur on day 8 of HDBR (HDT08, 125.41 ± 10.90µm, $p = 0.007$) as well as on day 29 (HDT29, 126.80 ± 10.05µm, $p = 0.011$) compared to day 1 (HDT01, 131.52 ± 10.85µm). Compared to the baseline (BDC-2, 130.40 ± 9.53µm) only HDT08 shows a significant decrease in vascular diameter ($p = 0.015$). Fig. IV.1 summarizes changes in CRAE ± SD over time.

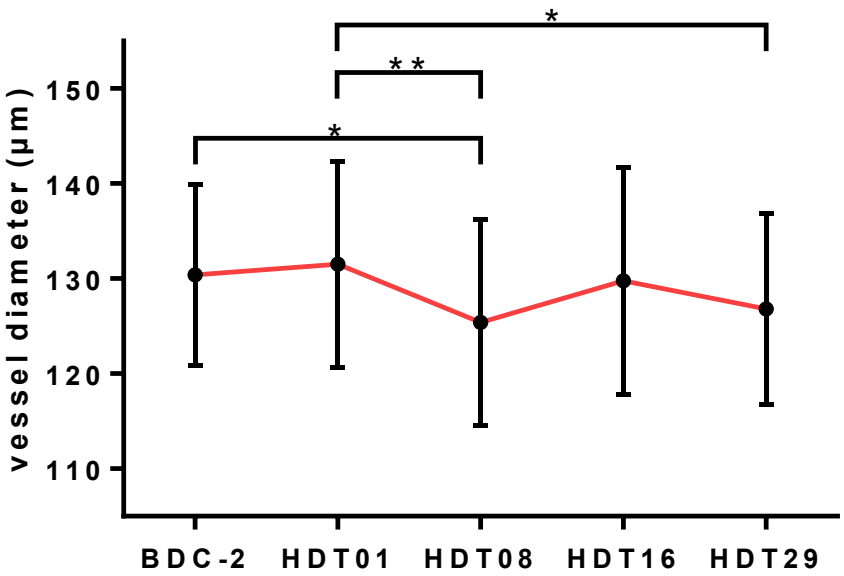

Fig. IV.1: CRAE (±SD) over time
BDC baseline data collection, HDT head-down tilt
(*) $p < 0.05$, (**) $p < 0.01$

IV.2 Central retinal vein equivalent

CRVE represents the mean diameter of the subjects' central retinal veins. The mean CRVE was 197.07 ± 13.56 µm. Table 5 lists the subjects' values for each time point.

Table 5: CRVE of subjects (values in µm)

Time point	A	B	C	D	E	F	G	H	I	J
BDC-2	172,32	188,63	197,14	193,63	228,90	192,77	186,41	209,22	206,57	203,67
HDT01	177,16	185,09	197,21	203,30	212,61	200,08	185,93	210,77	213,39	212,36
HDT08	170,02	187,48	198,06	200,30	211,56	176,97	191,38	205,80	199,71	203,41
HDT16	178,80	191,72	193,23	213,29	215,98	194,33	188,13	223,96	210,63	202,67
HDT29	165,92	181,64	184,87	200,47	203,54	192,67	190,33	204,60	199,82	195,06

CRVE data show an overall decrease in vessel diameter of 6.03 µm over the course of the study. A statistically significant decrease happens on day 29 (HDT29) of bedrest (191.89 ± 11.90µm, $p = 0.003$) compared to day 1 (HDT01, 199.79 ± 13.20µm). There is a decrease in CRVE on HDT08 co-aligning with CRAE data. As opposed to arterial diameter however, the decrease in venous diameter is statistically not significant ($p = 0.077$).

Fig. IV.2 summarizes changes in CRVE ± SD over time.

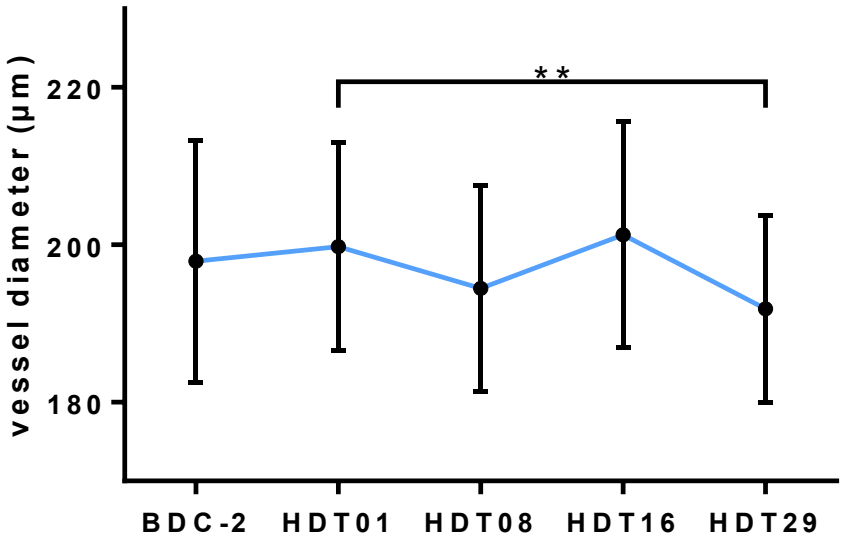

Fig. IV.2: CRVE (±SD) over time
BDC baseline data collection, HDT head-down tilt
(**) $p < 0.01$

IV.3 Arterio-venous ratio

AVR represents the ratio between the arteries' average diameter with respect to the average diameter of the veins. The mean AVR was 0.65 ± 0.04. Table 6 lists the subjects' AVR for each time point as calculated from CRAE and CRVE.

Table 6: AVR for subjects

Time point	A	B	C	D	E	F	G	H	I	J
BDC-2	0,733	0,708	0,597	0,669	0,571	0,654	0,649	0,731	0,646	0,652
HDT01	0,721	0,679	0,602	0,650	0,629	0,602	0,662	0,730	0,650	0,665
HDT08	0,696	0,656	0,615	0,640	0,610	0,663	0,578	0,733	0,615	0,650
HDT16	0,689	0,680	0,670	0,622	0,646	0,614	0,578	0,687	0,619	0,644
HDT29	0,715	0,671	0,638	0,677	0,646	0,613	0,613	0,716	0,629	0,694

There have been no significant changes in AVR throughout the study.

Figure IV.3 summarizes changes in AVR over time.

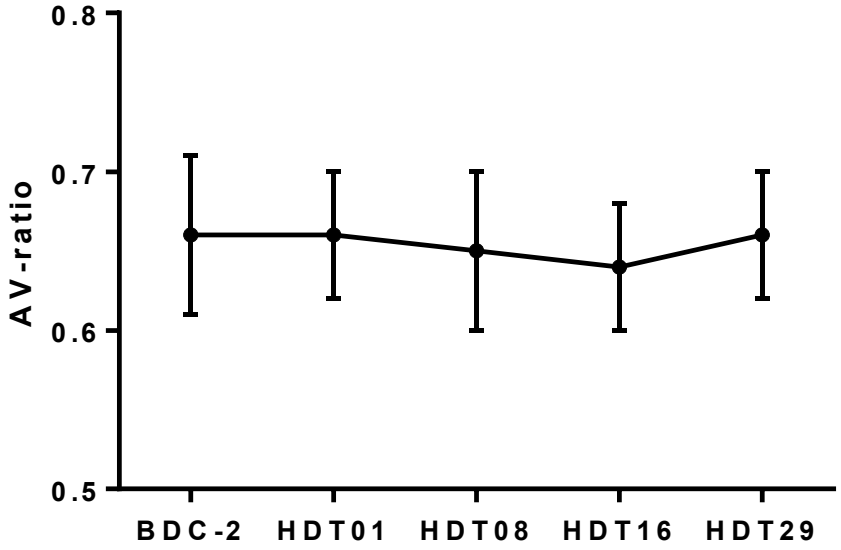

Fig. IV.3: AVR (±SD) over time
BDC baseline data collection, HDT head-down tilt

IV.4 Variability in individual subject's results

Looking at the individual subject's vessel diameters presents a very heterogeneous picture. While four subjects showed a net decrease in both CRAE and CRVE, two subjects displayed a net increase in both vessel diameter equivalents. Three subjects had an increase in CRAE while CRVE decreased and in one subject arterial equivalent decreased while venous equivalent increased. In sum half of the subjects' CRAE decreased while seven out of ten subjects showed a decrease in CRVE.

See figures VII.1 to VII.10 in the appendix for a graphical representation of CRAE and CRVE for subjects A to J.

V. DISCUSSION

The data shows that long term 6° head-down tilt bedrest has a measureable effect on central retinal vessel diameter. Both CRAE and CRVE decrease significantly over the course of the study. These results suggest that retinal imaging can be a useful tool for studying changes within the eye's microvascular network in bedrested subjects. It is non-invasive and easy to implement compared to other methods such as FMD.

V.1 Retinal vascular diameter, blood pressure and HDBR

Previous studies have shown that central retinal vessel diameter correlates inversely with systolic blood pressure (SBP) [50, 51]. Compared to healthy subjects, patients with hypertension have a significantly lower retinal arterial diameter [50], and their arterio-venous ratio is significantly reduced [52]. This shows that variations in blood pressure play a major role in retinal vascular adaptation, especially in changes of arterial diameter. During HDBR blood pressure is known to change. Short-term bedrest of only a couple hours to a few days has shown to increase mean arterial blood pressure (MAP) [53, 54]. During long-term bedrest, however, MAP showed no change or was even lower than pre-bedrest [55, 56]. This is most likely an effect of reduction of plasma volume during LTBR reducing overall load on the cardiovascular system.

The data reported in this diploma thesis do not show any significant changes of retinal vessel diameter on the first day of bedrest compared to baseline measurements. This might be because measurements on HDT01 were taken too early for any measureable effects of HDBR, such as fluid shift and increased hydrostatic pressure, to take place. On HDT08, after a week of bedrest, there is a significant decrease in CRAE as compared to HDT01. This could be explained by the vessels response to increased arterial pressure as CRAE has shown to be highly correlated with MAP [51]. The retinal vasculature greatly depends on local autoregulation to maintain blood flow. An increase in blood pressure might cause a myogenic response resulting in vasoconstriction. A recent study analyzing the effects of physical inactivity (using horizontal bedrest as simulation) on retinal vessels has shown that immobilization alone also causes CRAE to decrease significantly [57]. This suggests that the decrease in retinal equivalent cannot be attributed to increased pressures due to fluid shifts alone, but that systemic hormonal or metabolical changes possibly factor in as well. It has to be noted though that the change in posture and thus hydrostatic pressure during horizontal bedrest might be enough to trigger a myogenic response in retinal vessels

[57]. Monitoring and analyzing blood borne vasoactive agents during HDBR could grant further insights and make it possible to distinguish between local and systemic influences on microvascular changes during HDBR.

The increase in central retinal arterial equivalent on day 16 (HDT16) could be explained by reduction of plasma volume. The fluid shift towards the upper body during HDBR puts an increased load on the cardiovascular system, which will respond by increased diuresis. Subsequent reduction of plasma volume will reduce the load on the cardiovascular system and vessel diameters normalize. It is unclear if the amount by which CRAE increased can solely be explained by plasma volume reduction or if other factors (e.g. subjects' activities prior to measurement) might come into play. There was no plasma volume data obtained in this study so it is difficult to draw conclusions regarding the role of plasma volume changes on retinal vascular changes.

The central retinal vein equivalent shows fewer significant changes than the arterial diameter. I suspect this to be due to the structure of the vessel walls. The veins smooth musculature is not as strongly developed as that of arteries. Thus, they are less subject to vascular autoregulation, but rather passively adapt to blood flow and pressure. Although not measured directly, retinal blood flow presumably decreases because of the arterial narrowing as shown in the data. Changes in CRVE co-align with changes in arterial diameter, which supports the assumption of venous width being influenced by blood flow. Hydrostatic blood pressure is increased due to the cephalad fluid shift during head-down tilt, which should contribute to a widening of retinal veins. However, this effect might be counterbalanced by changes in intracranial and intraocular pressure.

V.2 Changes in retinal vascular function and intracranial pressure

Spaceflight has recently been implicated in the impairment of astronauts' visual perception, a condition known as visual impairment due to intracranial pressure (VIIP). Signs and symptoms include visual performance decrements, cotton wool spot formation, optic disc edema, choroidal fold development, optic nerve sheath distension or globe flattening [58]. These conditions present in varying degrees of severity and might even be permanent. Although the exact pathogenesis is still unclear it is believed that the primary cause for VIIP is a cephalad fluid shift in microgravity and the subsequent rise in intracranial pressure (ICP) and amount of cerebrospinal fluid (CSF) [58–60].

A study conducted recently showed that retinal vessel diameters not only follow changes in ICP but also depend on its baseline [61]. When lowering ICP through lumbar puncture both arterial and venous diameter decreased in subjects with normal ICP and increased when the subjects' baseline ICP was elevated [61]. Those findings suggest that there is an intricate balance between ICP and intraocular pressure (IOP) influencing central retinal vessel diameter.
Understanding these interconnections between intracranial pressure, intraocular pressure and retinal vascular function is paramount in preventing vision loss in astronauts. As discussed above, cephalad fluid shifts and subsequent rise in pressure might be a major factor in retinal vascular changes. It is advisable to perform retinal imaging during HDBR while at the same time measuring IOP and applying methods of non-invasively estimating ICP. This could shed more light on the matter and might even make it possible to quantify changes.

V.3 Clinical application of these findings

Cardiovascular deconditioning affects not only astronauts during long missions in space but also poses a challenge in the healthcare system and nursing homes, where patients are immobilized. Bedrest causes orthostatic intolerance in those patients, which prolongs their recovery and puts them at risk of falls. Retinal imaging can be used in a clinical setting to evaluate immobilized patients' vascular function and can help assessing the need for countermeasures and their effectiveness.

V.4 Limitations

It has to be noted that there are some limitations concerning the outcomes of this study. There were only ten subjects participating in this bedrest campaign. This is in part due to infrastructural limitations at the MEDES space clinic. However, the main reason for this low number of subjects is a financial one. Bedrest campaigns, especially long-term bedrest, are a costly endeavor. ESA only budgets and selects a few participants for those studies. With more generous funding, studies with larger sample sizes would be possible.

Because of the study's double-blinded design it was unknown which group, control (who only did the HDBR) or intervention (received LTBR-cocktail during HDBR), the subjects belonged to. At the time of writing this thesis, the subjects' affiliation to their respective groups has not yet been revealed. Any differences in central retinal vessel diameter can

thus not be linked to effects of the antioxidant-cocktail administered to the intervention group.

There was a large variability between individual subjects' results leading to a rather wide standard deviation. This might be because subjects vary in their cardiovascular reactions due to their anthropometrics (e.g. age or weight) or other factors still to uncover. However, it could also be attributed to the effects of the antioxidant countermeasure administered to some of the subjects. As pointed out above, which subject was allocated to which group (that is, bedrest with or without anti-oxidant therapy) was not known at the time of submission of this diploma thesis.

The last time point of data collection was on the 29th day of bedrest (HDT29). Due to unforeseen circumstances, even though the bedrest campaign was 60 days, I only had the retinal vessel data until the 29th day. It would be important for further studies to examine the long-term effects of bedrest confinement.

Additionally, there are some rather large gaps between data collection time points, the largest being 13 days passing between retinal imaging. A closer sequence of sampling points could provide more data and thus be more conclusive. However, in ESA sponsored studies this is not always possible due to time-schedules and several other ongoing projects.

It has to be considered that all of the subjects were males. The cardiovascular system of females is known to react differently to orthostatic challenges than that of males [62]. While men mostly react by adapting vascular resistance, women don't display this strong a vascular reaction but rather adapt their heart rate to maintain blood pressure. This is likely due to sex hormones' influence on the vascular system [63]. Because of differences in the menstrual cycle, considerable variations exist even between individual females [62]. The long-term bedrest study presented in this diploma thesis lasted 60 days and certainly would have included different menstrual phases. Therefore, to obtain comparable results of the effects of HDBR and the antioxidant-cocktail countermeasure across 60 days, only male subjects were chosen for this study. Future studies should incorporate females and take into account their menstrual phases. As retinal images are an important tool for the

assessment of vascular function, fundus photography could forward the understanding of gender differences in vascular health.

There might also be some considerable differences in vascular response throughout the year as well. This study was conducted in spring. Further studies at different times of the year might give provide varying information on changes in cardiovascular response throughout the seasons.

V.5 Conclusions and future directions

This novel study suggests that head down bedrest has a significant effect on central retinal vessel diameters which can be detected and analyzed using retinal imaging. Myogenic responses are the most likely cause for the decreases in central retinal artery and vein equivalent observed during this study.
To my knowledge no previous studies used fundus photography on subjects undergoing HDBR of sixty days. Fundus photography has proven to be very useful in non-invasively assessing vascular function and should be applied in future cardiovascular and spaceflight research as well as clinical medicine.

VI. REFERENCES

1. Creditor MC. Hazards of hospitalization of the elderly. Ann Intern Med. 1993;118:219–23.
2. Goswami N, Blaber AP, Hinghofer-Szalkay H, Montani J-P. Orthostatic intolerance in older persons: Etiology and countermeasures. Front Physiol. 2017;8:803. doi:10.3389/fphys.2017.00803.
3. Blaber AP, Landrock CK, Souvestre PA. Cardio-postural deconditioning: A model for post-flight orthostatic intolerance. Respir Physiol Neurobiol. 2009;169 Suppl 1:21-25. doi:10.1016/j.resp.2009.04.007.
4. Bate RR, Mueller DD, White JE. Fundamentals of astrodynamics. New York NY: Dover Publ; 1971.
5. National Aeronautics and Space Administration. Muscle atrophy. https://www.nasa.gov/pdf/64249main_ffs_factsheets_hbp_atrophy.pdf. Accessed 10 Mar 2018.
6. Akima H, Kawakami Y, Kubo K, Sekiguchi C, Ohshima H, Miyamoto A, Fukunaga T. Effect of short-duration spaceflight on thigh and leg muscle volume. Med Sci Sports Exerc. 2000;32:1743–7.
7. LeBlanc A, Rowe R, Schneider V, Evans H, Hedrick T. Regional muscle loss after short duration spaceflight. Aviat Space Environ Med. 1995;66:1151–4.
8. Orwoll ES, Adler RA, Amin S, Binkley N, Lewiecki EM, Petak SM, et al. Skeletal health in long-duration astronauts: Nature, assessment, and management recommendations from the NASA Bone Summit. J Bone Miner Res. 2013;28:1243–55. doi:10.1002/jbmr.1948.
9. Stein TP. Weight, muscle and bone loss during space flight: Another perspective. Eur J Appl Physiol. 2013;113:2171–81. doi:10.1007/s00421-012-2548-9.
10. National Aeronautics and Space Administration. Exploring space through math. https://www.nasa.gov/pdf/516064main_ALG_ED_BoneDensity%2012-23-10.pdf. Accessed 10 Mar 2018.
11. Campbell MR, Charles JB. Historical review of lower body negative pressure research in space medicine. Aerosp Med Hum Perform. 2015;86:633–40. doi:10.3357/AMHP.4246.2015.
12. Pavy-Le Traon A, Heer M, Narici MV, Rittweger J, Vernikos J. From space to Earth: Advances in human physiology from 20 years of bed rest studies (1986-2006). Eur J Appl Physiol. 2007;101:143–94. doi:10.1007/s00421-007-0474-z.

13. Zentrum für angewandte Raumfahrttechnologie und Mikrogravitation. The Bremen drop tower. https://www.zarm.uni-bremen.de/de/fallturm/allgemeine-informationen.html. Accessed 10 Mar 2018.
14. National Aeronautics and Space Administration. Zero gravity research facility. https://www1.grc.nasa.gov/facilities/zero-g/. Accessed 10 Mar 2018.
15. European Space Agency. European Space Agencies inaugurate altered-gravity aircraft. http://www.esa.int/Our_Activities/Human_Spaceflight/Research/European_space_agencies_inaugurate_altered-gravity_aircraft. Accessed 10 Mar 2018.
16. European Space Agency. Parabolic flights. http://www.esa.int/Our_Activities/Human_Spaceflight/Research/Parabolic_flights. Accessed 10 Mar 2018.
17. European Space Agency. Bedrest. 2013. http://esamultimedia.esa.int/multimedia/publications/Bedrest_Resting_for_science. Accessed 10 Mar 2018.
18. Jost PD. Simulating human space physiology with bed rest. Hippokratia. 2008;12 Suppl 1:37–40.
19. Brandes R, Busse R. Nerval vermittelte Durchblutungsregulation. In: Schmidt RF, Lang F, Heckmann M, editors. Physiologie des Menschen. 31st ed. Berlin: Springer; 2017. 593-596.
20. Brandes R, Busse R. Komponenten des basalen Gefäßtonus. In: Schmidt RF, Lang F, Heckmann M, editors. Physiologie des Menschen. 31st ed. Berlin: Springer; 2017. p. 596–598.
21. Grissmer S. Regulation der Organdurchblutung. In: Behrends JC, editor. Physiologie. 3rd ed. Stuttgart: Thieme; 2017. p. 154–159.
22. Brandes R, Busse R. Modulation des Gefäßtonus durch zirkulierende Hormone und vasoaktive Peptide. In: Schmidt RF, Lang F, Heckmann M, editors. Physiologie des Menschen. 31st ed. Berlin: Springer; 2017. p. 598–600.
23. Voets T, Nilius B. TRPCs, GPCRs and the Bayliss effect. EMBO J. 2009;28:4–5. doi:10.1038/emboj.2008.261.
24. Lüscher TF, Barton M. Biology of the endothelium. Clin Cardiol. 1997;20:II-3-10.
25. Cannon RO. Role of nitric oxide in cardiovascular disease: Focus on the endothelium. Clin Chem. 1998;44:1809–19.

26. Brandes R, Busse R. Das Endothel: zentraler Modulator vaskulärer Funktionen. In: Schmidt RF, Lang F, Heckmann M, editors. Physiologie des Menschen. 31st ed. Berlin: Springer; 2017. p. 600–607.
27. Luksha L, Agewall S, Kublickiene K. Endothelium-derived hyperpolarizing factor in vascular physiology and cardiovascular disease. Atherosclerosis. 2009;202:330–44. doi:10.1016/j.atherosclerosis.2008.06.008.
28. Kelm M. Flow-mediated dilatation in human circulation: Diagnostic and therapeutic aspects. Am J Physiol Heart Circ Physiol. 2002;282:H1-5. doi:10.1152/ajpheart.2002.282.1.H1.
29. Peretz A, Leotta DF, Sullivan JH, Trenga CA, Sands FN, Aulet MR, et al. Flow mediated dilation of the brachial artery: An investigation of methods requiring further standardization. BMC Cardiovasc Disord. 2007;7:11. doi:10.1186/1471-2261-7-11.
30. McClintic BR, McClintic JI, Bisognano JD, Block RC. The relationship between retinal microvascular abnormalities and coronary heart disease: A review. Am J Med. 2010;123:374.e1-7. doi:10.1016/j.amjmed.2009.05.030.
31. Wong TY, Hubbard LD, Klein R, Marino EK, Kronmal R, Sharrett AR, et al. Retinal microvascular abnormalities and blood pressure in older people: The Cardiovascular Health Study. Br J Ophthalmol. 2002;86:1007–13.
32. Bayrhuber H, Hauber W, Linder H, editors. Linder-Biologie. 23rd ed. Braunschweig: Schroedel; 2012.
33. Eysel U. Netzhaut – Aufbau, Signalaufnahme und Signalverarbeitung. In: Schmidt RF, Lang F, Heckmann M, editors. Physiologie des Menschen. 31st ed. Berlin: Springer; 2017. 358-364.
34. Paulsen F. WA. Auge und visuelles System. In: Zilles K, Tillmann B, editors. Anatomie. Berlin, Heidelberg: Springer-Verlag Berlin Heidelberg; 2010. 665ff.
35. Dauber W, Feneis H. Feneis' Bild-Lexikon der Anatomie. 10th ed. Stuttgart: Thieme; 2008.
36. Lüllmann-Rauch R, Asan E. Taschenbuch Histologie. 5th ed. Stuttgart, New York: Georg Thieme Verlag; 2015.
37. Frings S. MF. Netzhaut und primäre sensorische Prozesse. In: Behrends JC, editor. Physiologie. 3rd ed. Stuttgart: Thieme; 2017. 639-643.
38. Quigley HA, Brown AE, Morrison JD, Drance SM. The size and shape of the optic disc in normal human eyes. Arch Ophthalmol. 1990;108:51–7.

39. Trepel M. Neuroanatomie: Struktur und Funktion. 5th ed. München: Elsevier Urban & Fischer; 2012.
40. Fruttiger M, Calver AR, Krüger WH, Mudhar HS, Michalovich D, Takakura N, et al. PDGF mediates a neuron-astrocyte interaction in the developing retina. Neuron. 1996;17:1117–31.
41. Stone J, Dreher Z. Relationship between astrocytes, ganglion cells and vasculature of the retina. J Comp Neurol. 1987;255:35–49. doi:10.1002/cne.902550104.
42. Bhuiyan A, Lamoureux E, Nath B, Ramamohanarao K, Wong TY. Retinal image matching using hierarchical vascular features. Comput Intell Neurosci. 2011;2011:749054. doi:10.1155/2011/749054.
43. West H, Richardson WD, Fruttiger M. Stabilization of the retinal vascular network by reciprocal feedback between blood vessels and astrocytes. Development. 2005;132:1855–62. doi:10.1242/dev.01732.
44. MEDES Institute for Space Medicine and Physiology. The space clinic. http://www.medes.fr/en/the-space-clinic/the-infrastructure.html. Accessed 28 Mar 2018.
45. Teasell R, Dittmer DK. Complications of immobilization and bed rest. part 2: Other complications. Can Fam Physician. 1993;39:1440-2, 1445-6.
46. Dittmer DK, Teasell R. Complications of immobilization and bed rest. part 1: Musculoskeletal and cardiovascular complications. Can Fam Physician. 1993;39:1428-32, 1435-7.
47. Parr JC, Spears GF. General caliber of the retinal arteries expressed as the equivalent width of the central retinal artery. Am J Ophthalmol. 1974;77:472–7.
48. Hubbard LD, Brothers RJ, King WN, Clegg LX, Klein R, Cooper LS, et al. Methods for evaluation of retinal microvascular abnormalities associated with hypertension/sclerosis. Ophthalmology. 1999;106:2269–80.
49. Knudtson MD, Lee KE, Hubbard LD, Wong TY, Klein R, Klein BEK. Revised formulas for summarizing retinal vessel diameters. Curr Eye Res. 2003;27:143–9.
50. Chew SKH, Xie J, Wang JJ. Retinal arteriolar diameter and the prevalence and incidence of hypertension: A systematic review and meta-analysis of their association. Curr Hypertens Rep. 2012;14:144–51. doi:10.1007/s11906-012-0252-0.
51. Zhu P, Huang F, Lin F, Li Q, Yuan Y, Gao Z, Chen F. The relationship of retinal vessel diameters and fractal dimensions with blood pressure and cardiovascular risk factors. PLoS ONE. 2014;9:e106551. doi:10.1371/journal.pone.0106551.

52. Schuster AK-G, Fischer JE, Vossmerbaeumer C, Vossmerbaeumer U. Optical coherence tomography-based retinal vessel analysis for the evaluation of hypertensive vasculopathy. Acta Ophthalmol. 2015;93:e148-53. doi:10.1111/aos.12509.
53. Bonde-Petersen F, Suzuki Y, Sadamoto T, Christensen NJ. Cardiovascular effects of simulated zero-gravity in humans. Acta Astronaut. 1983;10:657–61.
54. Sun X-q, Pavy-LeTraon A, Gharib C. Change of cerebral blood flow velocity during 4 d head-down tilt bed rest. Space Med Med Eng (Beijing). 2002;15:163–6.
55. Voogel AJ, Stok WJ, Pretorius PJ, van Montfrans GA, Langewouters GJ, Karemaker JM. Circadian blood pressure and systemic haemodynamics during 42 days of 6 degrees head-down tilt. Acta Physiol Scand. 1997;161:71–80. doi:10.1046/j.1365-201X.1997.00203.x.
56. Zuj KA, Edgell H, Shoemaker JK, Custaud MA, Arbeille P, Hughson RL. WISE 2005: Responses of women to sublingual nitroglycerin before and after 56 days of 6° head-down bed rest. J Appl Physiol. 2012;113:434–41. doi:10.1152/japplphysiol.00445.2012.
57. Louwies T, Jaki Mekjavic P, Cox B, Eiken O, Mekjavic IB, Kounalakis S, Boever P de. Separate and combined effects of hypoxia and horizontal bed rest on retinal blood vessel diameters. Invest Ophthalmol Vis Sci. 2016;57:4927–32. doi:10.1167/iovs.16-19968.
58. Mader TH, Gibson CR, Pass AF, Kramer LA, Lee AG, Fogarty J, et al. Optic disc edema, globe flattening, choroidal folds, and hyperopic shifts observed in astronauts after long-duration space flight. Ophthalmology. 2011;118:2058–69. doi:10.1016/j.ophtha.2011.06.021.
59. Zhang L-F, Hargens AR. Spaceflight-induced intracranial hypertension and visual impairment: Pathophysiology and countermeasures. Physiol Rev. 2018;98:59–87. doi:10.1152/physrev.00017.2016.
60. Alperin N, Bagci AM. Spaceflight-induced visual impairment and globe deformations in astronauts are linked to orbital cerebrospinal fluid volume increase. Acta Neurochir Suppl. 2018;126:215–9. doi:10.1007/978-3-319-65798-1_44.
61. Moss HE, Vangipuram G, Shirazi Z, Shahidi M. Retinal vessel diameters change within 1 hour of intracranial pressure lowering. Transl Vis Sci Technol. 2018;7:6. doi:10.1167/tvst.7.2.6.
62. Barnes JN. Blood pressure regulation in women - differences emerge when challenged by orthostasis. J Physiol (Lond). 2013;591:2239. doi:10.1113/jphysiol.2013.254011.

63. Wenner MM, Haddadin A'S, Taylor HS, Stachenfeld NS. Mechanisms contributing to low orthostatic tolerance in women: The influence of oestradiol. J Physiol (Lond). 2013;591:2345–55. doi:10.1113/jphysiol.2012.247882.

VII. APPENDIX

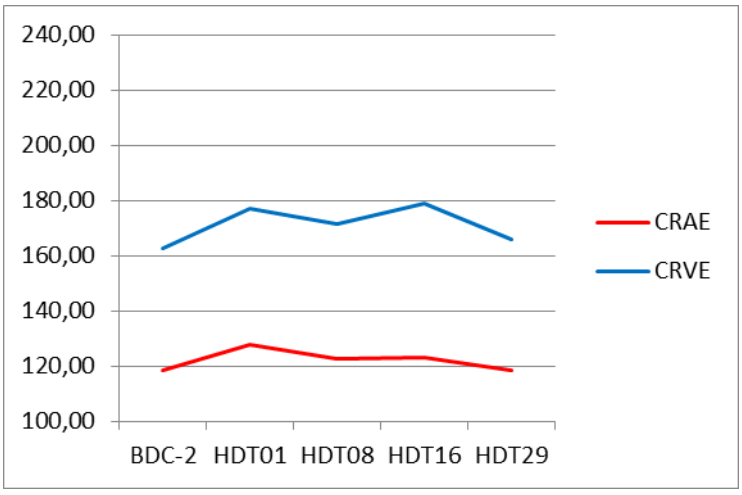

Fig. VII.1: Vessel diameter equivalents for subject A

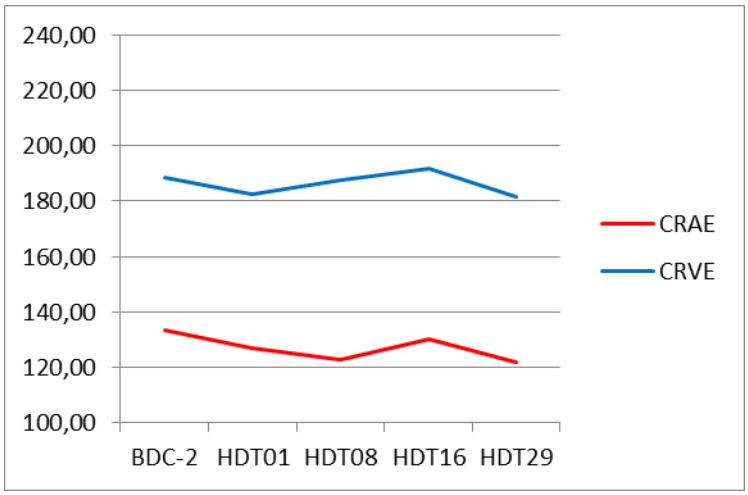

Fig. VII.2: Vessel diameter equivalents for subject B

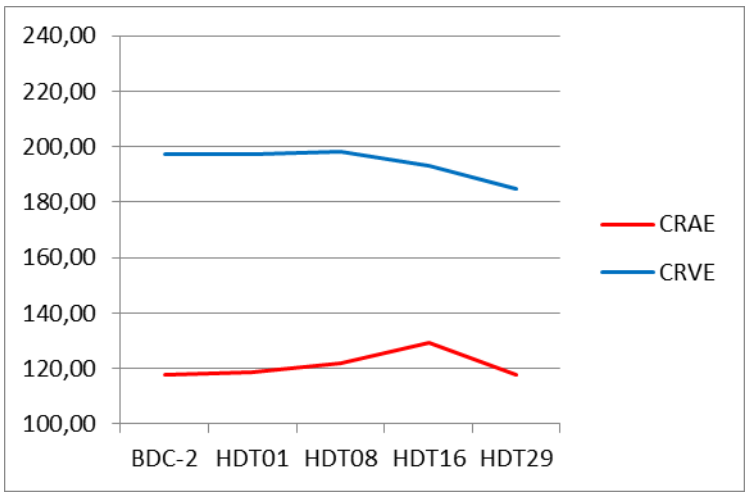

Fig. VII.3: Vessel diameter equivalents for subject C

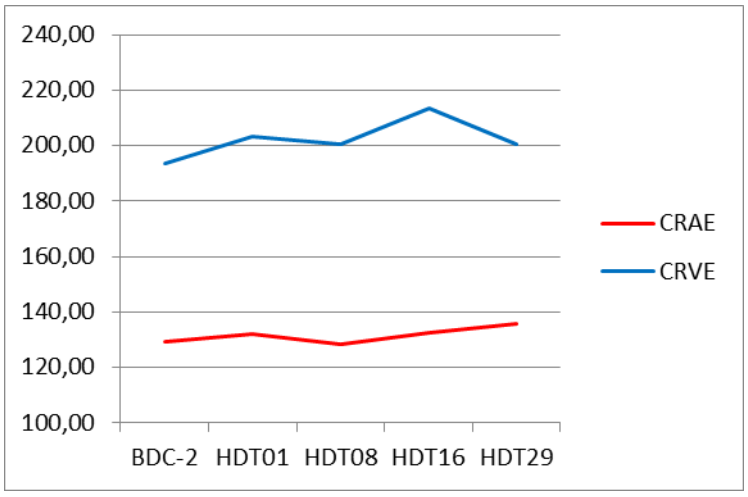

Fig. VII.4: Vessel diameter equivalents for subject D

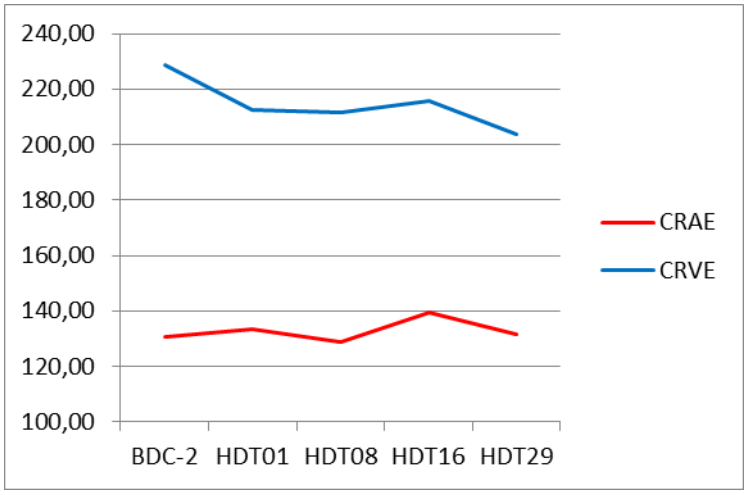

Fig. VII.5: Vessel diameter equivalents for subject E

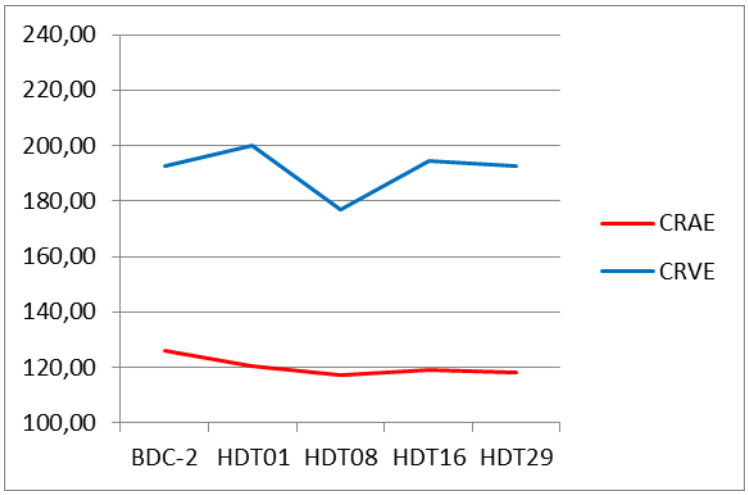

Fig. VII.6: Vessel diameter equivalents for subject F

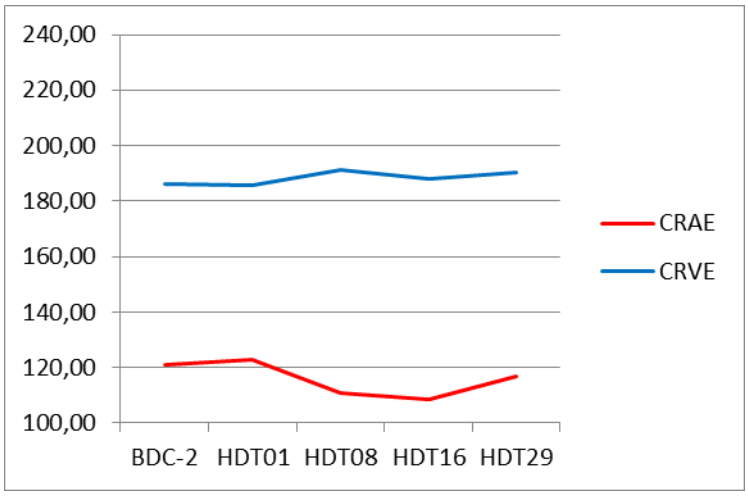

Fig. VII.7: Vessel diameter equivalents for subject G

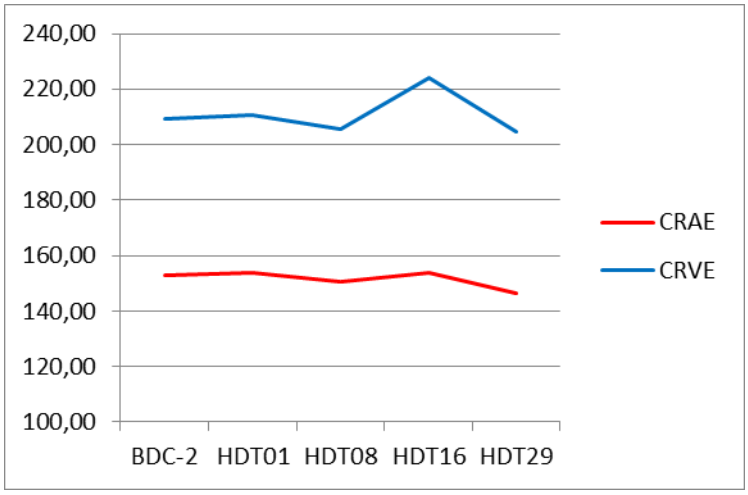

Fig. VII.8: Vessel diameter equivalents for subject H

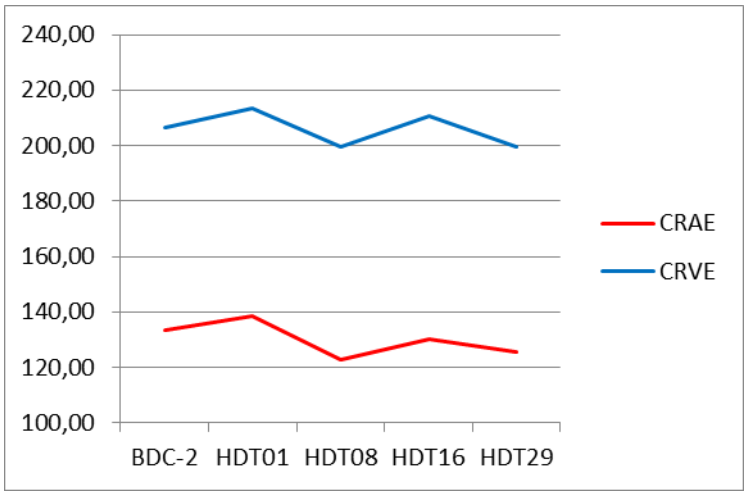

Fig. VII.9: Vessel diameter equivalents for subject I

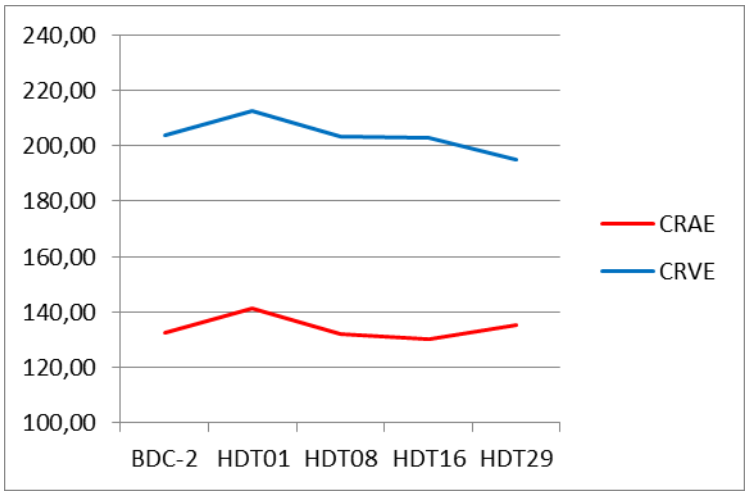

Fig. VII.10: Vessel diameter equivalents for subject J